

Renormalization Group calculations with k_k dependent couplings in a ladder

G. Abramovici, J. C. Nickel and M. Heritier

Laboratoire de Physique des Solides, associ   au C.N.R.S.,
Universit   de Paris Sud, Centre d'Orsay 91405 Orsay France

We calculate the phase diagram of a ladder system, with a Hubbard interaction and an interchain coupling t_\perp . We use a Renormalization Group method, in a one loop expansion, introducing an original method to include k_k dependence of couplings. We also classify the order parameters corresponding to ladder instabilities. We obtain different results, depending on whether we include k_k dependence or not. When we do so, we observe a region with large antiferromagnetic fluctuations, in the vicinity of small t_\perp , followed by a superconducting region with a simultaneous divergence of the Spin Density Waves channel. We also investigate the effect of a non local backward interchain scattering: we observe, on one hand, the suppression of singlet superconductivity and of Spin Density Waves, and, on the other hand, the increase of Charge Density Waves and, for some values of t_\perp , of triplet superconductivity. Our results eventually show that k_k is an influential variable in the Renormalization Group flow, for this kind of system.

PACS numbers: 71.10.Li, 71.10.Pm, 71.10.Fd, 74.20.-z, 74.20.Mn, 74.20.Rp

1. INTRODUCTION

The physics of ladder systems remains a source of considerable interest. In the last decades, many conductors were found, with anisotropic two-leg electronic structure, such as SrCu_2O_3 [1] or $\text{Sr}_{14-x}\text{Ca}_x\text{Cu}_2\text{O}_{41}$ [2] compounds. The structure of $\text{La}_2\text{Cu}_2\text{O}_5$ [3] can also be analyzed as weakly coupled ladders, and is therefore very similar. The phase diagram of these compounds is very rich; it is now well established that these systems behave like Luttinger liquids at high temperature, while they can behave like Fermi liquids when T decreases; they exhibit superconducting (SC) phases of type II, which can also be mixed with antiferromagnetic fluctuations. In some case, the SC phase is found to be spin-gapped, while spinless phases are also reported [4].

From a theoretical point of view, the ladder (or two-coupled chain) model is the simplest quasi-one-dimensional one. Although all its properties are not entirely elucidated, it has been used by many authors as a toy model, to build and explore new approaches (two-leaf dispersion models calculated by a Kadano-Wilson renormalization method [5] or by a bosonization method [6]; transition between commensurate and incommensurate filling [7], in particular close to the half-filling case [8, 9]; dimensional transition [10], etc.). These systems have been intensively used to investigate non conventional SC process (with singlet [11, 12, 13] or triplet [14] pairing).

This paper is devoted to the study of a ladder model, with a Hubbard interaction (U is the Hubbard constant) and an interband coupling (t_\perp is the interaction factor), at zero temperature. We investigate the phase diagram in the range of parameter $0 < U < 8 t_\perp$ and suppose that the electronic filling is incommensurate. Although there is yet no evidence for the existence of compounds lying in this range of parameter, we have hopes that some of these will indeed be found and confirm the theoretical predictions that we present here.

The phase diagram of this system has been partially studied by several authors. In particular, M. Fabrizio have used a Renormalization Group (RG) method, in a two-loop expansion from the Fermi liquid solution [12]. He includes interband backward scattering g_b , and, within the range of parameter that we have investigated, finds a SC phase, named 'phase I', which he clearly points out not to be singlet s, although he did not elucidate the symmetry of the condensate. In his calculations, the RG flow of susceptibilities shows several divergences: the Spin Density Wave (SDW) channel coexists with the superconducting one. This author did alternatively cut the flow before the divergences and bosonize the effective Hamiltonian; then, SDW modes disappear and are replaced by Charge Density Wave (CDW) instabilities.

These results are more or less compatible with that of other methods, using a one-loop expansion [15, 16], or bosonizing the Hamiltonian of the bare system [17, 18, 19, 20] (see also Ref. [13]), or using Quantum Monte Carlo method [21]. These authors generally find a singlet superconducting condensate of symmetry d, which coexists with SDW or CDW instabilities. This complicated phase has also been related to the RVB phase [22]. One of the central question is whether the SC modes are spin-gapped or not, and receives various and even contradictory answers. Using a two-loop expansion, Kishine [23] observes a spin gap, which is suppressed when $t_\perp \rightarrow 0$. This is also the result found with a Density Matrix RG method by Park [24].

We give a new insight into these questions, using a RG method, in a perturbative expansion in U . This kind of method has been used in many recent and very complete works [25, 26, 27]. Here, we calculate RG equations with one loop diagrams, including g_b couplings, as in Ref. [12], as well as all parallel momentum dependence.

Let us emphasize that, although we begin from the Fermi liquid solution, we find a phase with only SDW fluctuations, for small enough interband interaction $t_\perp < t_\perp(U)$, contrary to all previous results obtained by RG

methods, which always indicate SC instabilities as soon as $t_2 \neq 0$ (see for instance Lin et al. [15]). However, this phase is different from the one-dimensional limit. This is a very remarkable result, since k_k is known to be an irrelevant variable of the RG flow [28]. However, we will prove in this paper that it is indeed irrelevant in the very case of a ladder.

When t_2 is increased, we observe a transition at t_{2c} to a superconducting phase, where singlet SC instabilities of symmetry d coexist with SDW ones. This phase is found by many authors (see Refs. [12, 15, 16] and other articles already quoted).

Recently, Bourbonnais et al. [29, 30] have examined the effect of interchain Coulomb interactions for an infinite number of coupled chains, using RG method. Interchain backward scattering was found to enhance CDW fluctuations and favor triplet instead of singlet SC. We here investigated the effect of a Coulomb interchain backward interaction C_{back} for the ladder problem. We find that this interaction favors triplet SC instabilities instead of singlet ones and CDW instabilities instead of SDW ones in a ladder system too. Indeed, both the singlet SC and SDW instabilities (if any) are suppressed when C_{back} is increased, and we observe triplet SC as well as CDW instabilities. The triplet SC existence region is however very narrow and lies inside the region $t_2 < t_{2c}(U)$. For large values of C_{back} ($C_{back} \rightarrow U$), CDW is always dominant; this is consistent with what Lin et al. find [15].

On the contrary, when a Coulombian interchain forward interaction C_{for} is added, all SC instabilities are depressed, and we only observe SDW and CDW fluctuations.

We also present a detailed classification of the pair op-

erators in a ladder, which are connected to the order parameters. It proves a very powerful tool in these sophisticated RG methods.

So, we will first give a short description of the model (in section 2), then present the classification of the pair operators (in section 3, the symmetries are explained in appendix C), then we explain the RG formulation and techniques that are used here (in section 4). Results concerning only initially local interactions are presented in section 5, while those concerning the influence of additional interchain interactions are given in section 6. In section 7 we conclude.

2. MODEL

The Hubbard model of a ladder has been studied in various articles. We give here a brief presentation of this model (see Refs. [12] or [31] with similar notations).

a. Kinetic Hamiltonian

1. The model in a 1-d representation

The dispersion curve separates into two bands (0 and π), so the Fermi surface splits into four points (k_{F0} , k_F , k_F , k_{F0} in the k direction, + corresponds to right moving particles and - to left moving ones). The bands are linearized around the Fermi vectors [32] with a single Fermi velocity v_F (cf. Fig. 1). We write R the right moving particles and L the left moving ones. Then, the kinetic Hamiltonian writes

$$H_{cin} = \sum_{\mathbf{k}} v_F (\mathbf{k} - k_{F0}) R_0^\dagger (\mathbf{k}) R_0 (\mathbf{k}) + \sum_{\mathbf{k}} (\mathbf{k} - k_F) R^\dagger (\mathbf{k}) R (\mathbf{k}) + \sum_{\mathbf{k}} (\mathbf{k} + k_{F0}) L_0^\dagger (\mathbf{k}) L_0 (\mathbf{k}) + \sum_{\mathbf{k}} (\mathbf{k} + k_F) L^\dagger (\mathbf{k}) L (\mathbf{k}) : \quad (1)$$

We define the Fermi surface gap $k_F = k_{F0} - k_F$. One then gets $k_F = 2t_2/v_F$. The discretization step in k direction is a , and the reciprocal vector in this direction is defined modulo $2\pi/a$. The distance between the chains in z direction is b .

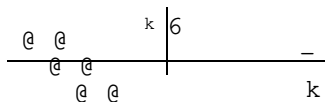


Figure 1: The 2-band dispersion in k direction

2. The model in a 2-d representation

The general 2-d dispersion law writes

$$\epsilon(\mathbf{k}) = 2t_k \cos(k_x a) - 2t_b \cos(k_y b)$$

as represented in Fig. 2; if one writes approximately $k_F = k_{F0} - k_F$, one gets $v_F = 2at_k \sin(k_F a)$. In real

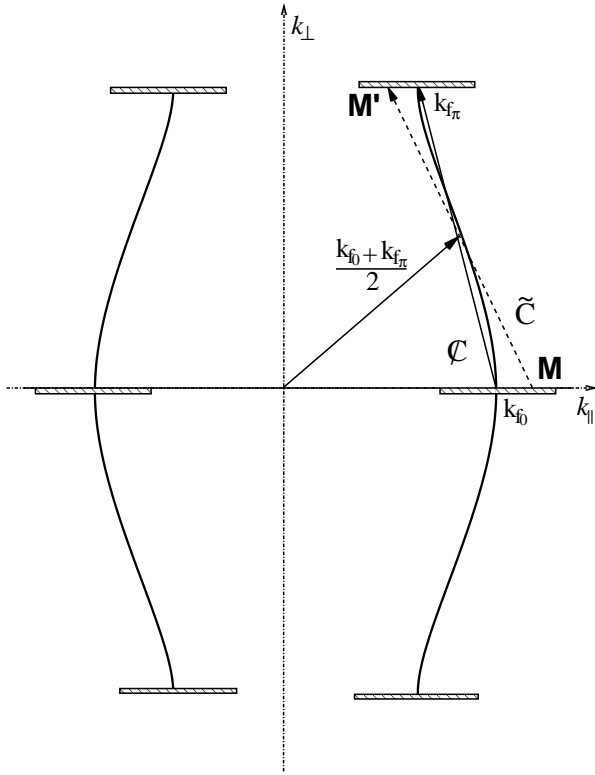


Figure 2: Two-dimensional representation of the states. The physical space, for a ladder, is restricted to the hatched bands at $k_{\perp} = 0$ and $k_{\perp} = \frac{\pi}{b}$. The curves correspond to the Fermi surface of a 2-d system, with an infinite number of chains. The four Fermi points, in the ladder system, are the intersections of these curves with the physical bands. The symmetry \tilde{C} that maps point M onto M' is the point symmetry around the Γ point, corresponding to $\frac{k_{f0} + k_f}{2}$. The symmetry \tilde{C} is the translation by the vector $k_{f0} - k_f$, which is also represented by a plain arrow.

space, y_k corresponds to the axis along the chains, and y_k takes only two values, $y_k = \pm 1$, corresponding to which chain one refers to. The k axis is then discretized, $y_k = 1/N$, where $4N$ is the total number of states. The Fourier transformation from real space functions to reciprocal space ones is detailed in appendix D.

From $y_k = \pm 1$, one gets $k_y = 0$ or $\frac{\pi}{b}$ ($k_y = \frac{\pi}{b}$ and $k_y = -\frac{\pi}{b}$ are identified). Therefore, the physical states are limited to the four horizontal bands, shown on Fig. 2, which are centered on each of the four Fermi points. The two bands centered on $(k_{f0}; 0)$ are the left and right bands (L_0 or R_0), the two bands centered on $(k_f; \frac{\pi}{b})$ are the left and right bands (L_{π} or R_{π}).

b. Interaction Hamiltonian

The most general interaction Hamiltonian can be written, with $L_k = L_0(K)$ for $k = (K; 0)$, $L_k = L_{\pi}(K)$ for $k = (K; \frac{\pi}{b})$ and idem for R ,

$$H_{\text{int}} = \frac{1}{N} \sum_{\substack{k_1, k_2; k_1^0, k_2^0 \\ k_1 + k_2 = k_1^0 + k_2^0}} \sum_{i, j} G_1(k_1; k_2; k_2^0; k_1^0) R_{k_1-1}^y L_{k_2-2}^y R_{k_1-1} L_{k_2-2} + G_2(k_1; k_2; k_2^0; k_1^0) R_{k_1-1}^y L_{k_2-2}^y L_{k_2-2} R_{k_1-1} \quad (2)$$

where G is the two-particle coupling, and we have used the g-ology representation. We do not include umklapp interactions G_3 ($L L R R$ or $R R L L$) nor G_4 terms ($L L L L$ or $R R R R$). We will alternatively use the singlet-triplet representation, where τ takes values $\pm s; t$, or the Charge-Spin representation, where $\tau = C; S$. If not necessary, we will omit the spin dependence. Eqs. (4) and (5) give, in appendix A, the usual relations between these different representations.

We distinguish, following Fabrizio [12], g_0 , which corresponds to $R_0^y L_0^y L_0 R_0$ process, g ($R^y L^y L R$), g_{f0} ($R_0^y L^y L R_0$), g_f ($R^y L_0^y L_0 R$);

g_{t0} ($R_0^y L_0^y L R$), g_t ($R^y L^y L_0 R_0$), g_{b0} ($R_0^y L^y L_0 R$) and g_b ($R^y L_0^y L R_0$). The definitions of these couplings, including the k_k dependence are detailed in A and Fig. 18; from symmetry considerations, one only needs g_0, g, g_{f0}, g_{t0} and g_{b0} ; in fact, we will see that even g can be deduced from g_0 in the very case of a ladder, so that we only deal with four couplings.

Bare couplings Of course, in the initial Hubbard model, the two-particle couplings do not depend on the momenta. We will define $U = U_a = (v_f)$ and $g = g_a = (v_f)$, to get rid of the physical dimensions. Then, the bare couplings values are simply $g_i = U$.

$O_s^{(s)}$ component corresponds to an interband pairing, named $-$ condensate ($Q = (k_f; \frac{\pi}{b})$), corresponding to z_+^{SC} , see A b) and writes

$$O_s^{(s)}(\mathbf{r}) = \frac{1}{2} \sum_{\mathbf{i}} e^{-k_f \cdot \mathbf{r}_i} \psi_{i1}^* \psi_{i1\#} + \psi_{i1}^* \psi_{i1\#} \\ = -\frac{1}{L} \sum_{\mathbf{p}} \frac{adp}{2} L_{p;0}^* R_{k_f(1\ 1)\ \mathbf{p};\#} + L_{p;0}^* R_{k_f(1\ 1)\ \mathbf{p};0\#} \\ + R_{k_f(1\ 1)\ \mathbf{p};0} L_{p;0} + R_{k_f(1\ 1)\ \mathbf{p};\#} L_{p;0\#};$$

it is however antisymmetric with parity ($P O_s^{(s)}(\frac{\mathbf{r}}{b}) = O_s^{(s)}(\frac{\mathbf{r}}{b})$); this comes from the $e^{-Q \cdot \mathbf{r}} = 2$ factor in the Fourier calculation, see details in D.

The s condensates are local in real space, see Fig. 3 (a).

If \mathbf{r} is replaced by $i_1 i_0 + j_1 j_0$, one gets extended s states (in reciprocal space variables, the components are multiplied by $\cos(\mathbf{p} \cdot \mathbf{a})$ or some similar factor, see some examples in D). However, we did not include these in our calculations.

3. Singlet d and g condensates

There are also two singlet condensates of d and g symmetry.

With $\mathbf{r} = i_1 i_0 + j_1 j_0$ (interchain pairing, with equal positions on each chain), one gets another pair operator. $O_s^{(d)}$ component is zero for singlet condensate, while $O_t^{(0)}$ component corresponds to an intraband pairing (0 -condensate) of d symmetry, and writes

$$O_s^{(d)}(0) = \frac{1}{2} \sum_{\mathbf{i}} \psi_{i1}^* \psi_{i1\#} + \psi_{i1}^* \psi_{i1\#} \\ = \frac{1}{L} \sum_{\mathbf{p}} \frac{adp}{2} L_{p;0}^* R_{p;0\#} + L_{p;0}^* R_{p;\#} \\ + R_{p;0} L_{p;0\#} + R_{p;\#} L_{p;\#};$$

With $\mathbf{r} = i_1 i_0 + j_1 j_0$, one gets a more complicated pair operator. $O_s^{(g)}$ component corresponds to an interband pairing ($-$ condensate) of g symmetry, and writes

$$O_s^{(g)}(\mathbf{r}) = \frac{1}{2} \sum_{\mathbf{i}} e^{-k_f \cdot \mathbf{r}_i} \psi_{i1}^* \psi_{i+1;1\#} + \psi_{i1}^* \psi_{i+1;1\#} \\ = e^{-\frac{k_f \cdot \mathbf{a}}{2}} \frac{1}{L} \sum_{\mathbf{p}} \frac{adp}{2} \sin(\mathbf{p} \cdot \mathbf{k}_{f0} + \frac{k_f}{2}) \\ L_{p-k_f;\#} R_{k_f-p;0\#} + R_{k_f-p;0} L_{p-k_f;\#} \\ + L_{p;0} R_{k_f(1\ 1)\ \mathbf{p};\#} + R_{k_f(1\ 1)\ \mathbf{p};0} L_{p;0\#};$$

be careful that the symmetry of the 0 -condensate is $d_{x^2-y^2}$ (i.e. it changes sign with C , see the definition afterwards), while that of the

$-$ condensate is both d_{xy} (i.e. it changes sign with p_x and p_y) and $d_{x^2-y^2}$; moreover, $d_{x^2-y^2}$ is imperfect on the $-$ condensate (for instance, it maps a factor $\sin(\mathbf{p} \cdot \mathbf{k}_{f0} + \frac{k_f}{2})$ onto $\sin(\mathbf{p} \cdot \mathbf{k}_{f0} + \frac{k_f}{2})$), which

slightly differs); however, the signs change according to g symmetry. A real space representation of the different condensates of singlet symmetry is given in Fig. 3.

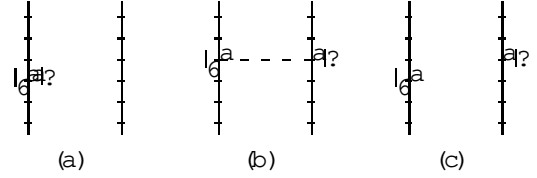


Figure 3: Real space representation of SC condensates of singlet symmetry (a), d (b) and g (c)

If the components, in reciprocal variables, are multiplied by $\cos(\mathbf{p} \cdot \mathbf{a})$ (or some similar factor), one gets extended d condensates (this corresponds to the harmonic classification).

4. Triplet condensates

One also finds triplet instabilities.

$O_t^{(p_x)}(0)$ corresponds to the p_x symmetry; $O_t^{(p_x)}(0)$ corresponds to an intraband pairing (0 -condensate), and writes

$$O_t^{(p_x)}(0) = \frac{1}{2} \sum_{\mathbf{i}} \psi_{i1}^* \psi_{i+1;1\ 0} + \psi_{i1}^* \psi_{i+1;1\ 0} \\ = \frac{1}{L} \sum_{\mathbf{p}} \frac{adp}{2} L_{p;0}^* R_{p;0\ 0} \\ + L_{p-k_f;\#} R_{k_f-p;0} \sin(\mathbf{p} \cdot \mathbf{k}_{f0})_{0\ 0};$$

$O_t^{(p_x)}(\mathbf{r})$ corresponds to an interband pairing ($-$ condensate), and writes

$$O_t^{(p_x)}(\mathbf{r}) = \frac{1}{2} \sum_{\mathbf{i}} e^{-k_f \cdot \mathbf{r}_i} \psi_{i1}^* \psi_{i+1;1\ 0} + \psi_{i1}^* \psi_{i+1;1\ 0} \\ = e^{-\frac{k_f \cdot \mathbf{a}}{2}} \frac{1}{L} \sum_{\mathbf{p}} \frac{adp}{2} L_{p;0}^* R_{k_f(1\ 1)\ \mathbf{p};0} \\ + L_{p-k_f;\#} R_{k_f-p;0} \sin(\mathbf{p} \cdot \mathbf{k}_{f0} + \frac{k_f}{2})_{0\ 0};$$

be careful that, because of the factor $e^{-Q \cdot \mathbf{r}} = 2$ in the Fourier transform, this condensate is invariant under P .

With $\mathbf{r} = i_1 i_0 + j_1 j_0$, one gets an intraband pairing (0 -condensate) of symmetry f_x , given by the $O_t^{(f_x)}(0)$ component

$$O_t^{(f_x)}(0) = \frac{1}{2} \sum_{\mathbf{i}} \psi_{i1}^* \psi_{i+1;1\ 0} + \psi_{i1}^* \psi_{i+1;1\ 0} \\ = \frac{1}{L} \sum_{\mathbf{p}} \frac{adp}{2} L_{p-k_f;\#} R_{k_f-p;0} \\ + L_{p;0} R_{p;0\ 0} \sin(\mathbf{p} \cdot \mathbf{k}_{f0})_{0\ 0};$$

note that $d_{x^2-y^2}$ is again in perfect.

With $\psi = \psi_0 e^{i\mathbf{k} \cdot \mathbf{r}}$, one gets an interband pairing (condensate) of symmetry f_y , given by the $O_t^{(f_y)}$ component

$$O_t^{(f_y)}(\mathbf{r}) = \frac{1}{L} \sum_{\mathbf{p}} e^{-i\mathbf{k} \cdot \mathbf{r}} \frac{1}{2} \sum_{\mathbf{p}'} L_{\mathbf{p};0} R_{\mathbf{k}-\mathbf{p};0} \psi_{\mathbf{p}} \psi_{\mathbf{p}'} = -\frac{1}{L} \sum_{\mathbf{p}} L_{\mathbf{p};0} R_{\mathbf{k}-\mathbf{p};0} \psi_{\mathbf{p}} \psi_{\mathbf{p}'} ;$$

note that p_y antisymmetry is an internal one and does not account on the exponential factor, in the Fourier transform. A real space representation of the different condensate of triplet symmetry is given in Fig. 4.

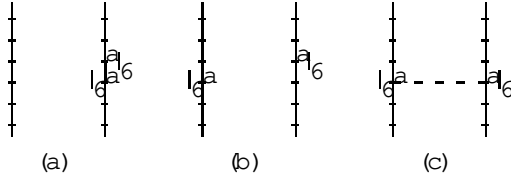


Figure 4: Real space representation of SC condensate of triplet symmetry p_x (a), f_x (b) and f_y (c)

Extended states of the same symmetries can be obtained exactly the same way as for singlet superconducting operators.

b. Density wave instabilities

1. DW Hamiltonian

We have also investigated site density waves instabilities, defined by the order parameter $P_{\text{site}}^{\text{DW}}(\mathbf{X}) = \langle \psi_{\mathbf{X}}^y; \mathbf{X}; 0 \rangle$, with $\mathbf{C} = \mathbf{I}$ for CDW, and $S_x = x$, $S_y = y$ and $S_z = z$, for SDW, as well as bond density waves instabilities, defined by the order parameter $P_{\text{bond}}^{\text{DW}}(\mathbf{X}) = \langle \psi_{\mathbf{X}}^y; \mathbf{X} + \mathbf{l}_k; 0 \rangle$, where $\mathbf{l}_k = (1; 0)$. These couplings are intrachain, we distinguish intraband and interband ones. We also investigated interchain couplings, defined by the order parameters $P_{\text{site}}^{\text{DW}}(\mathbf{X}) = \langle \psi_{\mathbf{X}}^y; \mathbf{X} + \mathbf{G}; 0 \rangle$ and $P_{\text{bond}}^{\text{DW}}(\mathbf{X}) = \langle \psi_{\mathbf{X}}^y; \mathbf{X} + \mathbf{G}; 0 \rangle$, where \mathbf{G} or $\mathbf{G} \pm 2\mathbf{l}_1$; $\mathbf{l}_1 + \mathbf{l}_2$ and $\mathbf{l}_2 = (0; 1)$.

The corresponding Hamiltonian writes, in reciprocal space variables,

$$H_{\text{DW}} = \sum_{\mathbf{p}} \sum_{\mathbf{p}'} Z^{\text{DW}}(\mathbf{p}; \mathbf{p}'; \mathbf{Q}) \psi_{\mathbf{p}}^y \psi_{\mathbf{p}'}^y + \sum_{\mathbf{p}} \sum_{\mathbf{p}'} Z^{\text{DW}}(\mathbf{p}; \mathbf{p}'; \mathbf{Q}) \psi_{\mathbf{p}}^y \psi_{\mathbf{p}'}^y : \quad (4)$$

The construction of the response functions for these instabilities is very similar to that of the superconducting instabilities. So, we will only give the Fourier components of the electron-hole pair operator for $Q = (2k_f; 0)$, $Q = (2k_f; 0)$ and $Q = (k_f; k_f)$.

SDW and CDW operators only differ by the spin factor (matrix or \mathbf{I}), so we will also omit this factor.

2. DW response function

The intraband response functions write then

$$O_{\text{site}}(2k_f; 0) = \frac{1}{L} \sum_{\mathbf{p}} \frac{\text{adp}}{2} R_{\mathbf{p};0}^y L_{\mathbf{p};0} + R_{\mathbf{p}+k_f;0}^y L_{\mathbf{p}+k_f;0} + R_{\mathbf{p}-k_f;0}^y L_{\mathbf{p}-k_f;0}$$

$$O_{\text{bond}}(2k_f; 0) = -\frac{1}{L} \sum_{\mathbf{p}} \frac{\text{adp}}{2} \sin(\mathbf{p} \cdot \mathbf{a}) e^{-i\mathbf{k}_f \cdot \mathbf{a}} (R_{\mathbf{p};0}^y L_{\mathbf{p};0} + R_{\mathbf{p}+k_f;0}^y L_{\mathbf{p}+k_f;0} + R_{\mathbf{p}-k_f;0}^y L_{\mathbf{p}-k_f;0})$$

and

$$O_{\text{site}}(2k_f; 0) = \frac{1}{L} \sum_{\mathbf{p}} \frac{\text{adp}}{2} R_{\mathbf{p}-k_f;0}^y L_{\mathbf{p}+k_f;0} + R_{\mathbf{p};0}^y L_{\mathbf{p};0} + R_{\mathbf{p}+k_f;0}^y L_{\mathbf{p}+k_f;0}$$

$$O_{\text{bond}}(2k_f; 0) = -\frac{1}{L} \sum_{\mathbf{p}} \frac{\text{adp}}{2} \sin(\mathbf{p} \cdot \mathbf{a}) e^{-i\mathbf{k}_f \cdot \mathbf{a}} (R_{\mathbf{p}-k_f;0}^y L_{\mathbf{p}+k_f;0} + R_{\mathbf{p};0}^y L_{\mathbf{p};0} + R_{\mathbf{p}+k_f;0}^y L_{\mathbf{p}+k_f;0}) :$$

The interband response function writes

$$O_{\text{site}}(k_f; k_f; \frac{\pi}{2}) = -\frac{1}{L} \sum_{\mathbf{p}} \frac{\text{adp}}{2} R_{\mathbf{p};0}^y L_{\mathbf{p};0} + R_{\mathbf{p};0}^y L_{\mathbf{p};0}$$

$$O_{\text{bond}}(k_f; k_f; \frac{\pi}{2}) = \frac{1}{L} \sum_{\mathbf{p}} \frac{\text{adp}}{2} e^{i\frac{\mathbf{k}_f \cdot \mathbf{a}}{2}} \sin(\mathbf{p} \cdot \frac{\mathbf{k}_f}{2}) (R_{\mathbf{p};0}^y L_{\mathbf{p};0} + R_{\mathbf{p}+k_f;0}^y L_{\mathbf{p}+k_f;0} + R_{\mathbf{p}-k_f;0}^y L_{\mathbf{p}-k_f;0}) :$$

The above response function are intrachain ones. The way we have written them one just needs to add a minus sign before the first (or second) term of all intrachain operators, to obtain all interchain ones.

4. RENORMALIZATION GROUP EQUATIONS

a. Choice of the RG scheme

We have used the One Particle Irreducible (OPI) scheme (Ref. [26, 33, 34]), to calculate all diagrams, in a one-loop expansion. We use the flow parameter $\ell = e^{-\ell}$. We do not renormalize v_f nor k_{f0} or k_f .

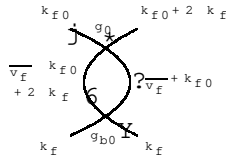
b. k_x dependent equations

1. k_x dependence of the couplings

In this system, the interband backward scattering g_b plays a particular role. Due to momentum conservation,

it is not possible to put all its arguments onto the Fermi points. This indicates that g_b is not a low energy process. However, it intervenes in the renormalization of low energy processes. For instance, in the renormalization of g_0 , $\frac{dg_0}{d\lambda}$ gives a contribution containing a g_{b0} scattering, with a factor $\frac{1}{v_F k_F}$. This contribution is exponentially suppressed, as $v_F k_F = 2t_z$. It can thus be neglected as soon as $v_F k_F$ is of the order or bigger than the initial bandwidth $2\phi_0$. On the other hand, as shown by Fabrizio [12], the g_b process has to be taken into account if $v_F k_F$ is much smaller than ϕ_0 .

Thereupon, in order to calculate the renormalization of g_{b0} properly, couplings g_0 , g_F or g_t with specific k_k dependence are needed. For instance, $\frac{dg_{b0}}{d\lambda}$ gives a Peierls diagram :



including coupling $g_0(k_{F0}; k_{F0} + 2k_F; k_{F0} + 2k_F; k_{F0})$, with arguments that remain separated from the Fermi points, even in the limit $\phi_0 \rightarrow 0$, let us write it g_{01} . This coupling separates from coupling $g_0(k_{F0}; k_{F0}; k_{F0}; k_{F0})$, with all arguments at the Fermi points, which we will write g_{00} ; therefore k_k dependence is irrelevant. This can be proved by comparing their renormalization, in the Cooper channel. For instance, $\frac{dg_{00}}{d\lambda}$ gives, in the Cooper channel, a term proportional to $g_0^2 + g_t^2$ with a constant factor, which is present all the way down to $\phi_0 \rightarrow 0$. On the contrary, $\frac{dg_{01}}{d\lambda}$ gives, in the Cooper channel, a term with a factor $\frac{2}{2 + v_F p_1 + p_2} = \frac{1}{v_F k_F}$; the renormalization of g_{01} in the Cooper channel is thus exponentially suppressed, when $\phi_0 \rightarrow 0$ (for g_{00} , the total incoming momentum is $p_1 + p_2 = 0$).

We have proved that different g_0 couplings separate during the flow, so the k_k dependence is hence capable to have an effect during the flow, when it is taken into account. This generalizes for g_F , g_t and even g_b couplings.

All this differs completely from the one-dimensional case, where the renormalization of the coupling with all momenta on the Fermi points is only governed by processes with momenta $k_F \pm \frac{\phi_0}{v_F}$, which always fall on the Fermi points when $\phi_0 \rightarrow 0$. In our case, it is not possible to apply the same argument as soon as $t_z \neq 0$. Indeed, we will see, in the following, that one gets different results, depending on whether we take the k_k dependence of the couplings into account or not.

The k_k dependence can be observed, when ϕ_0 is large (and till $\phi_0 > v_F k_F$), by the separation of the different scattering couplings g_0 , g_{F0} and g_{t0} . On the contrary, if one puts $g_b = 0$ at $\phi_0 = 0$, this dependence is suppressed, and the system becomes purely one-dimensional for small values of t_z (in that case, g_b remains 0 for all ϕ_0 and the

RG equations simplify drastically, although they differ from the one-dimensional case).

2. k_k representation of the couplings g

In order to write explicit k_k -dependent RG equations, one needs to define a consistent and detailed k_k representation of the couplings g .

Let us first note that $G(p_1; p_2; p_2^0; p_1^0)$ corresponds to $R^Y(p_1)L^Y(p_2)L(p_2^0)R(p_1^0)$, where p_i are the absolute momenta in the k direction. We then define the relative momenta $p_1 = p_1 - k_{F1}$, $p_2 = p_2 + k_{F2}$, $p_3 = p_3 + k_{F3}$ and $p_4 = p_4 - k_{F4}$, and write, correspondingly, $g(p_1; p_2; p_2^0; p_1^0)$. We also introduce variables $c = p_1 + p_2 = p_1^0 + p_2^0 + d$, $l = p_1 - p_1^0 = p_2^0 - p_2 + d$ and $p = p_1 - p_2^0 = p_1^0 - p_2 + d$, where $d = -2k_F$ for g_{b0} , $d = 2k_F$ for g_b , and d is zero otherwise, and then write, correspondingly, $g(c; l; p)$ (d is implicit).

At the beginning of this section, we have found in a diagram a particular coupling $g_0(\frac{1}{v_F}; 2k_F; 0; 2k_F + \frac{1}{v_F})$. When $\phi_0 \rightarrow 0$, we get $g_0(0; 2k_F; 0; 2k_F)$ (which also writes $g_0(2k_F; -2k_F; 0)$ in $(c; l; p)$ notation). Note that some arguments are shifted by $-2k_F$, compared to the coupling $g_0(0; 0; 0; 0)$ with all momenta on the Fermi points.

This could be easily generalized for all couplings g . So, in order to get a reasonable number of couplings, we have done the following approximation: all terms $\frac{1}{v_F}$, in all diagrams, are replaced by their $2k_F$ part (i.e. by $2k_F \frac{1}{2k_F v_F}$, where $[x]$ is the biggest integer $\leq x$). Then, it follows that we only get couplings $g(p_1; p_2; p_2^0; p_1^0)$ (or $g(c; l; p)$), where all variables p_i (or $c; l; p$) are multiples of $2k_F$.

3. k_k representation of the couplings z

All the preceding procedure generalizes to the couplings z as well.

We first introduce a $(k; c; p)$ representation, similarly, with $c = p_1 + p_2$, $p = p_2 - p_1$ and $k = p_1$, where p_1 and p_2 are defined on Fig. 19 and write, correspondingly, $z^{SC}(c; k)$ or $z^{DW}(p; k)$.

Then, we apply the same approximation in order to get couplings, where all variables $(k; c; p)$ are multiples of $2k_F$.

The same conclusion applies to these couplings, proving that their k_k dependence is also irrelevant.

4. RG equations

Finally, we calculate the RG flow of the separated following couplings: $g_0(0; 0; 0; 0)$,

$g_0(2k_f; 0; 0; 2k_f)$, $g_0(0; 2k_f; 0; 2k_f)$, etc. as well as $z(0; 0)$, $z(2k_f; 0)$, etc.

The exact RG equations, including all k components, are given in B a, for the $g(c; l; p)$, and in B b, for the $z^{SC}(c; k)$ and $z^{DW}(p; k)$.

In order not to solve an infinite number of equations, we have reduced the effective bandwidth of the renormalized couplings to $4n_{max}k_f$, where n_{max} is an integer, by projecting all momenta lying out of the permitted band, back into it, according to a specific truncation procedure that will be explained after.

We have performed our calculations with $n_{max} = 2, 3$ or 4, and the results rapidly converge as n_{max} is increased.

5. Susceptibility equations

To each instability corresponds a susceptibility. We will write $^{SC}()$ the different SC ones and DW the different SDW or CDW ones.

The susceptibilities have no k_k dependence. However, couplings z with different k_k variables appear in their RG equations, which we give in B c.

Referring to the transverse component of the interaction vectors, we will write (0) the instabilities corresponding to intraband processes, and (\pm) those corresponding to interband ones.

We use several symmetries, to reduce the number of couplings. Because of the k_k dependence, it is not as easy to apply them as in ordinary cases. We give here some indications, which are completed in appendix.

c. Symmetries

1. Ordinary symmetries

We apply C the conjugation symmetry ($C : r ! r; p ! p; !$), A the (antisymmetrical) exchange between incoming particles, A^0 the exchange between outgoing particles, P the space parity ($P : r ! r; p ! p; !$) and S the spin rotation ($S : !$). We will also use p_x, p_y (the mirror symmetries in the k and y directions), f_x and f_y . Note that $P = p_x p_y$.

H_{cin} (Eq. (1)) and H_{int} (Eq. (2)) satisfy all these symmetries, whereas SC instabilities, governed by H_{SC} (Eq. (3)), are not invariant under S or C, which allows a natural classification of the states, and DW instabilities, governed by H_{DW} (Eq. (4)), do satisfy CS, AS or A^0S , but not C, A, A^0 nor S symmetries.

All the relations satisfied by G or Z couplings are detailed in C a. From what precedes, one will not be surprised that those for G couplings are simpler and less sophisticated than those for Z ones.

Relations of couplings g We are not interested here in the symmetries that relate, for instance, a LRLR coupling to a RLLR one. Instead, we only keep RLLR couplings and deduce all the symmetries that keep this order.

We then apply them to every coupling g_0, g , etc., and find, altogether, exactly two independent relations for each one, which write, in $(c; l; p)$ notation,

$$\begin{aligned} g_i(c; l; p) &= g_i(c; l; p) \quad i = 0; \quad t; t = 9 \\ g_f(c; l; p) &= g_{f0}(c; l; p) \\ g_b(c; l; p) &= g_{b0}(c; l - 2k_f; p - 2k_f); \end{aligned} \quad (G-1)$$

$$\begin{aligned} g_i(c; l; p) &= g_i(c; l; p) \quad i = 0; \quad f; f = 9 \\ g_t(c; l; p) &= g_{t0}(c; l; p) \\ g_b(c; l; p) &= g_{b0}(c - 2k_f; l; p - 2k_f); \end{aligned} \quad (G-2)$$

One observes that G-1 relates g_{f0} to g_f and g_{b0} to g_b , while G-2 relates g_{t0} to g_t and g_{b0} to g_b . The combination of G-1 and G-2 thus relates g_{f0} to g_f and g_{t0} to g_t .

Relations of couplings z We similarly deduce all symmetries that keep the LR order; we apply them to every coupling z_0, z , etc., and find only one relation for each one, which writes, in $(k; c; p)$ notation,

$$\begin{aligned} z_s^{SC}(c; k) &= z_s^{SC}(c; k - c) = 0; \quad \geq 9 \\ z_{t0}^{SC}(c; k) &= z_{t0}^{SC}(c; k - c) \\ z_s^{SC}(c; k) &= z_{s+}^{SC}(c; k - c) \quad \geq \\ z_{t+}^{SC}(c; k) &= z_{t+}^{SC}(c; k - c) \end{aligned} \quad (Z-SC-1)$$

where \geq reads + for $= s$ or $= p_x$ and \geq for $= g$ or $= f_y$. Note that z_0^{SC} or s^{SC} correspond to intraband condensates, while z_{+}^{SC} or s^{SC} correspond to interband ones.

$$\begin{aligned} z^{DW}(p; k) &= z^{DW}(p; p - c) = 0; \\ z^{DW}(p; k) &= z^{DW}(p; p - c) \end{aligned} \quad (Z-DW-1)$$

where \geq reads + for site ordering and \geq for bond ordering.

One observes that Z-1 relates z_{+} to z .

2. Supplementary symmetry

As we already noted, ordinary symmetries do not relate g_0 to g , nor z_0 to z . However, since we choose identical bare values at $\lambda = 0$, and since the RG equations are symmetrical, we observe an effective symmetry between these couplings: we will show here that this does not occur by chance, but that it follows a specific symmetry C^* , which only applies to the ladder system.

C^* is a kind of conjugation: it generalizes the electron-hole symmetry as follows.

Let us first consider the case of a single band one-dimensional system; we find an electron-hole symmetry, described in Fig. 5 (a).

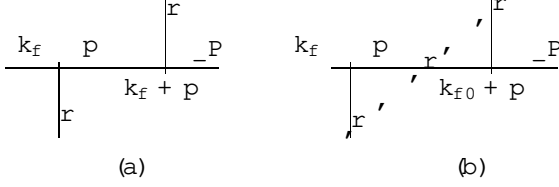


Figure 5: Symmetry around the Fermi points : (a) in a 1-band system ; (b) in a 2-band system

For R particles, it conjugates an electron with momentum $k_f + p$ and a hole with momentum $k_f - p$. In the momentum space, it is a symmetry around k_f . One can write $\mathcal{C}^p = \frac{y}{2k_f} p$ and $\mathcal{C}^y = \frac{y}{2k_f} p$. For L particles, the same relation applies if one simply changes k_f into k_f .

Let us now return to the two-band system. This symmetry generalizes by turning the momenta around the isobarycenter of the Fermi points, as shown in k space in Fig. 5 (b). For R particles, $(k_{f0} + k_f)/2$ points to the isobarycenter and you now get $\mathcal{C}^p = \frac{y}{k_{f0} + k_f} p$ etc.

In the two-dimensional representation, \mathcal{C} -symmetry is a point symmetry around $(\frac{k_{f0} + k_f}{2}; \frac{y}{2b})$, as shown on Fig. 2 (the sign depends on whether it is a R or L momentum).

Actually, there is an alternative symmetry, which we write \mathcal{G} , which also maps the band $k_y = 0$ onto the band $k_x = 0$: it is a translation by the vector $(\frac{k_f - k_{f0}}{2}; \frac{y}{2b})$, as shown on Fig. 2. Some of the bare couplings satisfy this \mathcal{G} symmetry (g_0, g_f, g_t, z_0 or z), but some don't (g_b, z_+ , z_-). Since interactions are mixing all couplings as soon as the flow parameter $\ell > 0$, the renormalized couplings will break the \mathcal{G} symmetry. Therefore, we can't use it.

On the contrary, one verifies that $H_{\text{cin}}, H_{\text{int}}, H_{\text{SC}}$ and H_{DW} are invariant under \mathcal{C} . The induced relations satisfied by G or Z couplings are detailed in C b.

In fact, \mathcal{C} and \mathcal{G} weakly correspond to the $d_{x^2-y^2}$ symmetry in two dimensions.

Supplementary relation of couplings g It is straightforward that \mathcal{C} keeps the RLLR order when one applies it to any coupling g_i ; so we find a new relation for each one, which writes, in $(c; l; p)$ notation,

$$\begin{aligned} g(c; l; p) &= g_0(c; l; p) \\ g_f(c; l; p) &= g_{f0}(c; l; p) \\ g_t(c; l; p) &= g_{t0}(c; l; p) \\ g_b(c; l; p) &= g_{b0}(c; l; p) \end{aligned} \quad (\text{G-3})$$

One verifies that g_0 and g are related; in fact, G-3 relates all 0-couplings to $-$ couplings.

Supplementary relation of couplings z Similarly, \mathcal{C} keeps LR order when we apply it to any coupling z_i ; so we find a new relation for each one, which writes, in $(k; c; p)$ notations,

$$\begin{aligned} z^{\text{SC}}(c; k) &= z_0^{\text{SC}}(c; k) \\ z^{\text{SC}}(c; k) &= z_4^{\text{SC}}(c; k) \end{aligned} \quad (\text{Z-SC-2})$$

where $+$ reads $+$ for s or p_x and $-$ for $d; g$ or $f_x; f_y$.

$$\begin{aligned} z^{\text{DW}}(p; k) &= z_0^{\text{DW}}(p; k) \\ z^{\text{DW}}(p; k) &= z_4^{\text{DW}}(p; k) \end{aligned} \quad (\text{Z-DW-2})$$

where $+$ reads $+$ for site ordering and $-$ for bond ordering.

Again, one verifies that z_0 and z_- are related (as well as z_+ and z_0).

d. Truncation

Understanding symmetry relations does not only help us to reduce drastically the number of couplings, it is also an essential tool to make a proper truncation procedure, as we will explain now.

1. Triplet notation

Let us first introduce a useful notation for the k_k dependence.

We have already defined the relative momentum representation $g(p_1; p_2; p_2^0; p_1^0)$, as well as the $g(c; l; p)$ notation, and explained how to keep only couplings, the arguments of which are all multiples of $2k_f$. We will focus on the $(c; l; p)$ notation and write $c = 2n_1 k_f$, $l = 2n_2 k_f$, $p = 2n_3 k_f$, with $(n_1; n_2; n_3) \in \mathbb{Z}^3$.

In short, we can write $g_i(n_1; n_2; n_3)$ ($i = 0; f; t; b$), where $(n_1; n_2; n_3)$ is called a triplet. Mind that, using symmetry relations, two triplets $(n_1; n_2; n_3)$ and $(n_1^0; n_2^0; n_3^0)$ can represent the same coupling. One says that these triplets belong to the same symmetry orbit (or symmetry class). Mind also that the orbits are different for each coupling g_0, g_{f0}, g_{t0} and g_{b0} .

It would take too long to give an exhausted list of these orbits. Let us just observe that $(0; 0; 0)$'s orbit has only one element (itself), except for g_b , the orbits of which we detailed in appendix C c.

2. Choice of the truncation procedure

Obviously, one needs only renormalize one coupling per orbit. From the fundamental rules, explained in 4b2, it follows that, even if one starts with only $g_0(0; 0; 0); g_{f0}(0; 0; 0)$ and $g_{t0}(0; 0; 0)$, the RG equations will generate an infinite number of orbits. So, we will only keep couplings which satisfy $|n_i| \leq n_{\text{max}}$ (for a given n_{max}); but even so, in the RG equations of some orbits intervene couplings, with arguments lying outside of the permitted band (i.e. the distance of the corresponding momentum to the Fermi point exceeds $2n_{\text{max}} k_f$). In order to get a consistent closed set of differential equations, one needs to put these extra couplings back, inside the set of allowed couplings.

For instance, imagine that $n_{\text{max}} = 2$, and that $g(3;2;2)$ coupling intervenes in a RG equation. One cannot, unfortunately, just map $(3;2;2) \rightarrow (2;2;2)$, because these triplets do not belong to the same symmetry orbit. In doing so, one would get a very poor k_k dependence; we have actually proved, in the case of a $(p_1; p_2; p_2^0)$ representation, that all orbits of g_0 except $(0;0;0)$ would collapse into one single orbit.

Therefore, the truncation procedure must be compatible with all the symmetries of the system. We have used the $(c;l;p)$ notation, which is very convenient. One can check that all the symmetries conserve $c + l + p \pmod{4k_f}$. This explains why $n_i \rightarrow n_i - 1$ can't be compatible with the symmetries. On the contrary, $n_i \rightarrow n_i - 2$ is completely compatible, i.e. it maps a triplet onto an already defined orbit; hence we have used this mapping for the extra couplings.

With $n_{\text{max}} = 2$, for each coupling we find 63 different couplings¹, which separate into 23 orbits (having 1, 2 or 4 elements), except for the g_0 couplings. For these, the enumeration is more tedious, we eventually find 8 orbits (of 4 elements, see C c). There are altogether $3 \times 23 + 8 = 77$ different orbits; if we include the spin separation, we thus need to calculate 154 coupled differential equations. $n_{\text{max}} = 3$ gives 390, while $n_{\text{max}} = 4$ gives 806.

e. Divergences of the susceptibilities

In the range of values for U that we have investigated, the RG flow is always diverging.

When the initial interaction Hamiltonian H_{int} is purely local, i.e. when the interchain scattering are discarded ($C_{\text{back}} = C_{\text{for}} = 0$), the interband SDW susceptibility $\chi_S^{\text{DW}}(\frac{\pi}{b})$ is always divergent. In the superconducting phase, the SC singlet d susceptibility $\chi_S^{\text{SC(d)}}(0)$ is also divergent, at the same critical scale $\ell_c = \ell_0 e^c$. A third susceptibility $\chi_S^{\text{DW}}(0)$ increases and reaches a high plateau (see Fig. 6). Almost all other susceptibilities remain negligible.

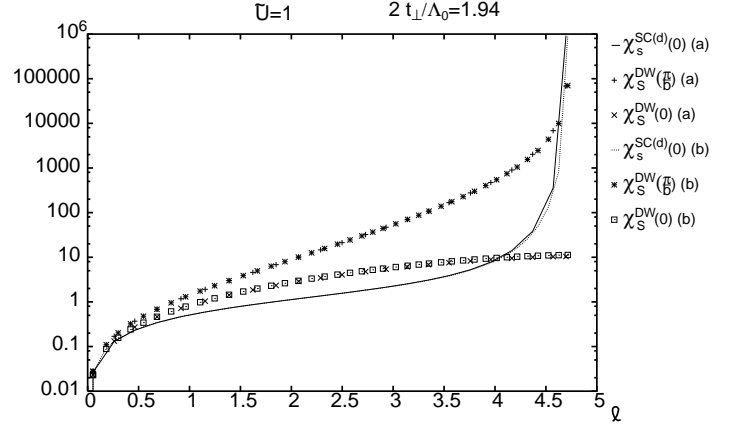


Figure 6: Flow of the susceptibilities $\chi_S^{\text{SC(d)}}$ and χ_S^{DW} (intra or interband), at $U = 1$ and $2t_{\perp}/\Lambda_0 = 1.94$: (a) usual RG procedure; (b) including k_k dependence. You observe that $\chi_S^{\text{DW}}(0)$ does not diverge but only reaches a plateau.

When the parameters C_{back} or C_{for} are increased, both $\chi_S^{\text{DW}}(\frac{\pi}{b})$ and $\chi_S^{\text{SC(d)}}(\frac{\pi}{b})$ decrease; they are progressively replaced by the divergence of the CDW susceptibility $\chi_C^{\text{DW}}(\frac{\pi}{b})$, and, in the case of backward scattering, of the triplet SC susceptibility $\chi_t^{\text{SC(f)}}(0)$.

One finds at most four divergent susceptibilities ($\chi_S^{\text{SC(d)}}(0)$, $\chi_C^{\text{DW}}(\frac{\pi}{b})$, $\chi_t^{\text{SC(f)}}(0)$ and $\chi_S^{\text{DW}}(\frac{\pi}{b})$) at a time.

Since the RG flow is diverging, we cannot further calculate the renormalized couplings. To deduce a phase diagram, we must find out which mechanism dominates; we used two different criteria: according to the first one, we simply take the susceptibility which reaches the highest value j at ℓ_c ; according to the second one, we take the susceptibility which has the highest slope.

These two criteria bring non equal results. Although the first one is a poorer criterion, its conclusions remain stable when either the precision or n_{max} are changed. The second is however preferred, as we will see its conclusion are physically consistent, contrary to the first one.

5. PHASE DIAGRAM WITH INITIALLY LOCAL INTERACTIONS

Let us first discuss the case of initially local interactions ($C_{\text{back}} = C_{\text{for}} = 0$, no interchain scattering). Of course, we can only see H_{int} at $\ell = 0$, and the flow will develop non local interactions.

a. Results

We begin with the phase diagram obtained when the k_k dependence is neglected.

¹ that are $f(i;j;k); i,j,k = 2;0;2g$ $f(1;1;i); i = 2;0;2g$ $f(1;i;1); i = 2;0;2g$ $f(i;1;1); i = 2;0;2g$

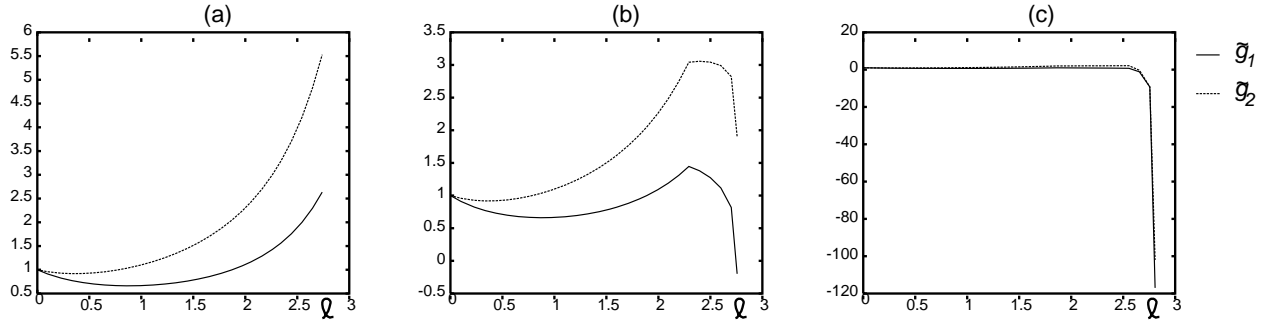


Figure 7: Flow of the couplings g_{01} and g_{02} at : (a) $t_2 = t_{2c}(U)$; (b) $t_2 = t_{2c}(U)$; (c) t_2 & $t_{2c}(U)$

1. Phase diagram with no k_k dependence

In the region of the phase diagram that we have investigated ($0 < U < 2$), the SC susceptibility $\chi_s^{SC(d)}(0)$ is always divergent, as well as the SDW susceptibility $\chi_s^{DW}(\frac{\pi}{b})$ (see Fig. 6).

According to the slope criterion, $\chi_s^{SC(d)}(0)$ always dominates. We induce that this region is superconducting (this is consistent with the conclusions of Fabrizio [12]), and that the pairing is of symmetry d ; however, the presence of SDW instabilities, developing in the same region, makes a detailed determination of this phase very uneasy and beyond the possibilities of our approach. We will call it SC phase.

2. Phase diagram with k_k dependence

SC phase When t_2 is large, we find similar results. For instance, with $U = 1$, there is no significant differences for $2t_2 = 0$ to 1.94 (see Fig. 6).

SDW phase On the contrary, the superconducting susceptibility is almost suppressed when t_2 is small enough. For $U = 1$ and $2t_2 = 0 = 0.016$, $\chi_s^{SC(d)}(0)$ is 5 orders of magnitude smaller than $\chi_s^{DW}(\frac{\pi}{b})$, at c , see on Fig. 8. In this phase, the SDW's instability develops so rapidly that it overwhelms all other processes. This indicates indeed a pure SDW phase.

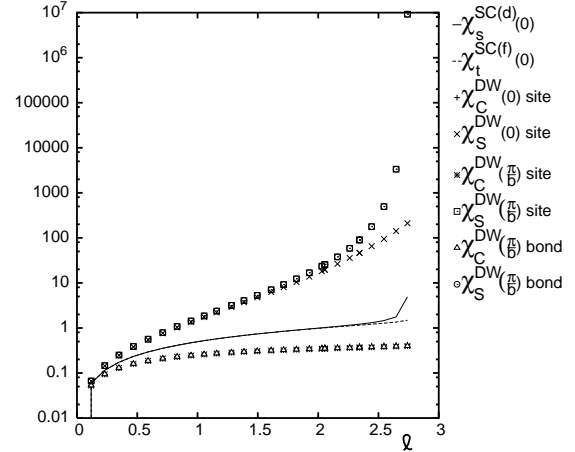


Figure 8: Flow of some susceptibilities, at $U = 1$ and $2t_2 = 0 = 0.016$. $\chi_s^{SC(d)}(0)$ is almost suppressed at c .

Hence, this result differs drastically from those obtained when the k_k dependence is neglected.

Moreover, we observe a transition between the SDW phase and the SC one, at a critical parameter $t_{2c}(U)$.

Critical behavior We characterize this transition by different ways.

First of all, the behaviour of the renormalized two-particle couplings change very rapidly, at $t_{2c}(U)$: as t_2 decreases, $g_{01}(c)$ and $g_{02}(c)$ shrink suddenly, then, after a little interval, $g_{01}(c)$ and $g_{02}(c)$ become positive (and even $> U$, see on Fig. 7). We also observe changes, though less significant, for the other couplings g (for instance, $g_{f01}(c)$ decreases and $g_{b1}(c)$ becomes negative when t_2 increases).

Moreover, we observe (on Fig. 9) a marked site/bond separation of the SDW susceptibility, at $t_{2c}(U)$. The site and bond SDW susceptibilities are degenerate for $t_2 = t_{2c}(U)$ (in the SDW phase), which is consistent with the fact they should be equal at $t_2 = 0$ (where the system is purely one-dimensional, see Ref. [35]), while they smoothly separate after the transition. The same site/bond separation occurs for the CDW susceptibility.

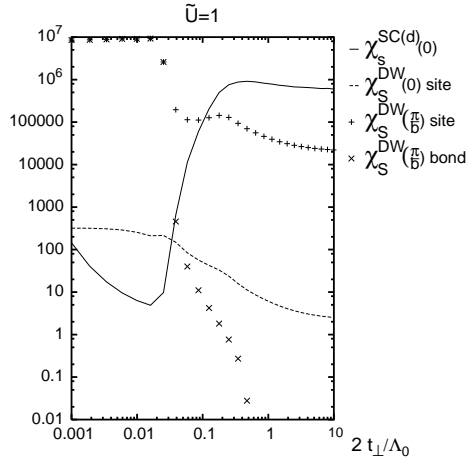


Figure 9: Curves of $\chi_S^{SC(d)}(\omega_c)$ and $\chi_S^{DW}(\omega_c)$ versus $2t_\perp/\Lambda_0$.

Transition region The behaviour of most of the parameters that we have examined indicates the same critical value $t_{\perp c}(U)$, which we have determined exactly, using the slope criterion.

However, $\chi_S^{SC(d)}(\omega_c) < \chi_S^{DW}(\pi/2)$ holds until t_\perp reaches a value $t_{\perp c2}(U)$; this second critical value, which corresponds to the height criterion, is confirmed by minor modifications of behaviour, which occur in the interval $t_{\perp c}(U) < t_\perp < t_{\perp c2}(U)$ and are very smooth (for instance, $\chi_{b1}(\omega_c)$ and $\chi_{b2}(\omega_c)$ cross).

The numerical determination of $t_{\perp c2}(U)$ is very stable (see Fig. 10), and the complete behaviour, from the SDW phase to the SC phase, is clear on Fig. 9, which shows the absolute values of the susceptibilities at ω_c .

The region $t_{\perp c}(U) < t_\perp < t_{\perp c2}(U)$ is called transition region, we believe it is a superconducting phase, where SDW instabilities seem however to dominate. The SDW are precursor manifestations of the pure SDW phase, which is next to the transition region.

As already stated, our results converge very rapidly when the band width on which we project the momenta is increased. The complete phase diagram (for $C_{back} = C_{for} = 0$) is shown on Fig. 10, for $n_{max} = 2; 3$ and 4.

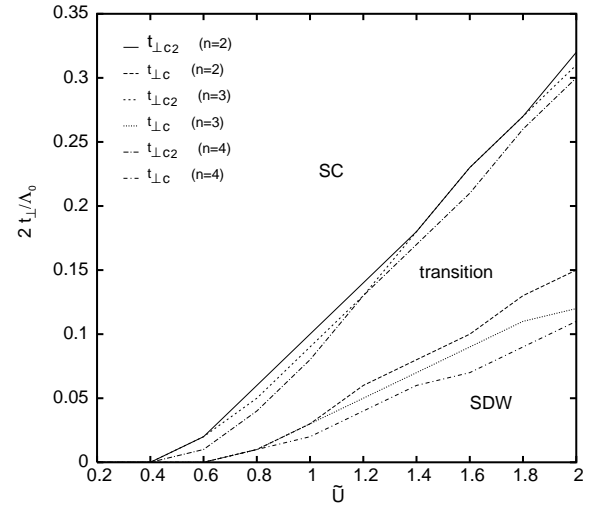


Figure 10: Phase diagram when the k_k dependence is included.

Moreover, it is most interesting to note that, contrary to the pure SDW phase, the transition region can be detected when the k_k dependence is neglected (the value of $t_{\perp c2}(U)$ is lowered). This can be seen, for instance, on Fig. 11, which corresponds to Fig. 9 with no k_k dependence.

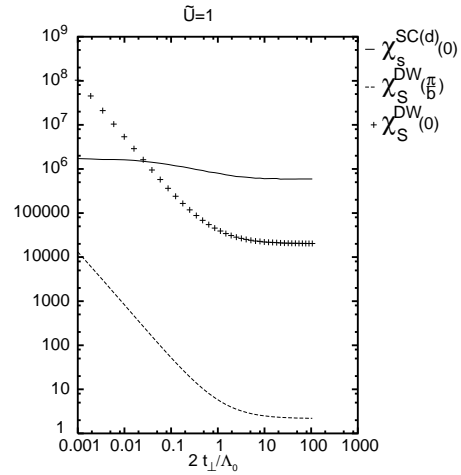


Figure 11: Curves of $\chi_S^{SC(d)}(\omega_c)$ and $\chi_S^{DW}(\omega_c)$ versus $2t_\perp/\Lambda_0$ when k_k is neglected.

SC critical temperature The critical energy ω_c at which SC susceptibility diverges gives an approximate indication of the SC critical temperature. We give a plot of $\omega_c = 0$ versus $2t_\perp/\Lambda_0$; as seen on Fig. 12, ω_c is roughly decreasing with t_\perp . The band gap parameter t_\perp is also increasing with pressure; therefore, this behaviour is compatible with the experimental data, which show that T_c is decreasing with pressure in quasi-one-dimensional organic compounds.

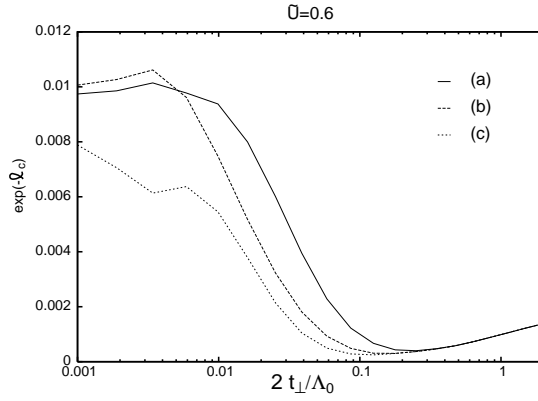


Figure 12: Curves of $\chi_c = 0 = e^{-\chi_c}$ versus $2t_2 = 0$ with $n_{max} = 2$ (a), $n_{max} = 3$ (b) and $n_{max} = 4$ (c).

b. Discussion

As already mentioned, as soon as the dependence of k_k is included, we observe two separated phases, one purely SDW, the other one a SC phase with competing SDW instabilities.

On the other hand, for $t_2 \ll 1$, i.e. when the initial bandwidth lies inside $[k_f; k_{f0}]$, the k_k dependence has no observable influence on the susceptibilities.

In the SDW phase, our results prove the existence of large antiferromagnetic fluctuations. We believe that these SDW instabilities are not the signature of a localized antiferromagnetic ground state, but of antiferromagnetic itinerant electrons, as it is indeed observed in Bechgaard salts. Actually, the flow is driving towards a fixed point, which does not seem to be the one-dimensional solution: for instance, the renormalized couplings g_1 and g_2 of the 1-d solution are 0 and 1/2 and differ from the values which we obtain when the flow is diverging, in the SDW phase (see Fig. 7 (a)).

We induce that the spin-gap should disappear in this SDW region, which is consistent with what Park and Kishine [23, 24] claim.

In the SC phase, the SC divergence is due to the Cooper channel, while that of density waves is due to the Peierls one (see, in the case of a single band model, Refs. [32, 36]). The appearance of d-wave superconductivity in ladder systems is well understood within a strong coupling scenario, where a spin gap leads to interchain Cooper pairing. However, in our calculations, we see that superconducting correlations are always enhanced by SDW fluctuations. Contrary to what Lee et al. claimed first [37], there is an itinerant electron mechanism in this case, which is the weak coupling equivalent of the localized electron mechanism in the strong electron scenario. It was proposed by Emery [38], and is essentially the spin analog of Kohn-Luttinger superconductivity. The mutual enhancement of the two channels is also discussed in Refs. [33, 39].

As a consequence of this mutual enhancement, the spin-gap should not appear with the first appearance of SC instabilities, but for somehow larger values of t_2 .

Moreover, we observe that the SC pairing is a $Q = 0$ mechanism, while the SDW are excited by $Q = (2k_f; \frac{\pi}{b})$ vectors. This can be explained by the symmetry of each channel. The Green function of the Cooper channel gives a factor $1 = (\mathbf{k}) + (\mathbf{k})$ and is minimized with the $k \rightarrow k$ symmetry, which corresponds to an intraband process. The Green function of the Peierls channel gives a factor $1 = (\mathbf{k}) + (\mathbf{k} + \mathbf{Q})$ and is minimized with the $k \rightarrow k + \mathbf{Q}$ symmetry, which corresponds to an interband process.

This can also be seen in the RG equations. $d \ln(z^{SC}(0)) = d\chi$ depends only on g_0 and g_t , whereas $d \ln(z^{SC}(\frac{\pi}{b})) = d\chi$ depends on g_f and g_b . Since g_b processes are depressed as soon as $2t_2, 0$ -condensate are favored. Moreover, this predominance is stabilized by the $dg_t = d\chi$ equations, in which the Cooper term depends on g_0 , and by the $dg_b = d\chi$ equations, in which the Cooper term depends on g_f .

The same argument applies for DW instabilities. $d \ln(z^{DW}(0)) = d\chi$ depends on g_0 and g_b , whereas $d \ln(z^{DW}(\frac{\pi}{b})) = d\chi$ depends on g_f and g_t . So, π -processes are favored. A gain, this is stabilized by the $dg_t = d\chi$ equations, in which the Peierls term depends on g_f , and by the $dg_b = d\chi$ equations, in which the Peierls term depends on g_0 .

The critical temperature, in the SC phases, is indicated in Fig. 12. We chose $U = 0.6$ in order to avoid the SDW phase. The general trend is that of a quasi-one-dimensional system; the increasing curve, for small values of t_2 , can be related to transition effect and to the furthered influence of the SDW fluctuations.

6. PHASE DIAGRAM WITH INITIAL COULOMBIAN INTERCHAIN SCATTERING

a. Results

1. Influence of a backward interchain scattering

Let us now study the effect of a backward interchain scattering. This type of coupling has been investigated by Bourbonnais et al. [29] in the context of correlated quasi-one-dimensional metals, for which CDW correlations are enhanced and triplet superconducting instabilities can occur. When the parameter C_{back} is increased, the behaviour of the susceptibilities depends on the parameters ($t_2; U$).

Appearance of triplet SC and CDW For $t_2 \ll t_c(U)$, the SDW phase exists for C_{back} small enough. As C_{back} is further increased, the SDW instabilities are replaced by CDW ones. The transition is smooth, and there is a narrow region where both SDW and CDW coexist (region 3 in Fig. 16). We show a $2t_2 = 0 = 0.01$ section of the susceptibilities at χ_c on Fig. 13.

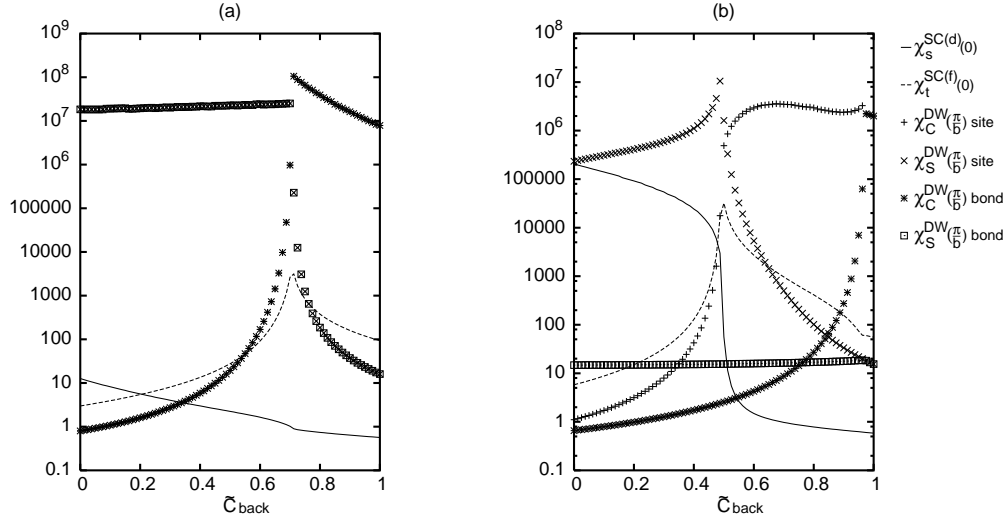


Figure 13: Curves of the χ versus C_{back} , at $U = 1$ and a) $2t_z = 0 = 0.01$; b) $2t_z = 0 = 0.1$.

For $t_z \leq t_{c_g}(U)$, the SC phase (with SC singlet d and SDW instabilities) exists for C_{back} small enough. As C_{back} is further increased, the singlet SC modes are replaced by triplet ones, while SDW are replaced by CDW. Singlet and triplet SC appear to be antagonistic, and the transition is very pronounced; in the coexistence line between them, one also finds SDW and CDW divergences (see Fig. 14). On the contrary, the transition between SDW and CDW is very smooth, although the coexistence region is still narrow (region 2 in Fig. 16). We show a $2t_z = 0 = 0.1$ section of the susceptibilities at t_c on Fig. 13.

When C_{back} is large enough, the triplet SC modes are suppressed, and the region is a pure CDW phase. We show a section of the susceptibilities at t_c , for $C_{back} = 0.2$ and $C_{back} = 0.3$, on Fig. 15, which clearly indicates the domain of existence of the triplet SC.

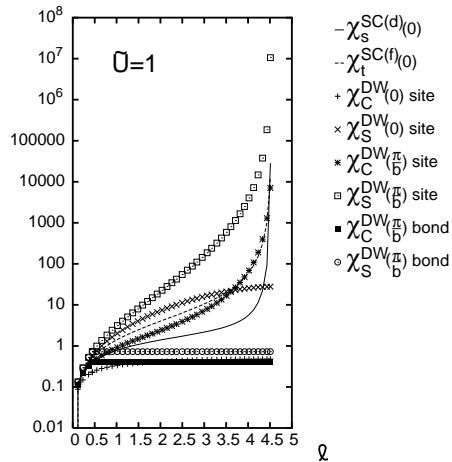


Figure 14: Flow of the susceptibilities for $2t_z = 0 = 0.32$ and $C_{back} = 0.18$.

The triplet SC condensate has f_x symmetry. The corresponding susceptibility is mostly divergent in a region of coexistence with SDW and CDW (region 2 in Fig. 16), but it is also divergent in a region of coexistence with only CDW (region 1 in Fig. 16).

Site/bond separation As we have already observed it, in the case of $C_{back} = C_{for} = 0$, for small values of t_z , site and bond SDW susceptibilities are degenerate, as well as site and bond CDW ones.

This generalizes for all values of C_{back} . The site/bond separation line is an increasing function $t_{zg}(C_{back})$ of C_{back} , shown on Fig. 16; For small values of U , this line crosses the SC domain, but for $U = 1$ it is already disconnected from the SC frontier (although it remains close to it).

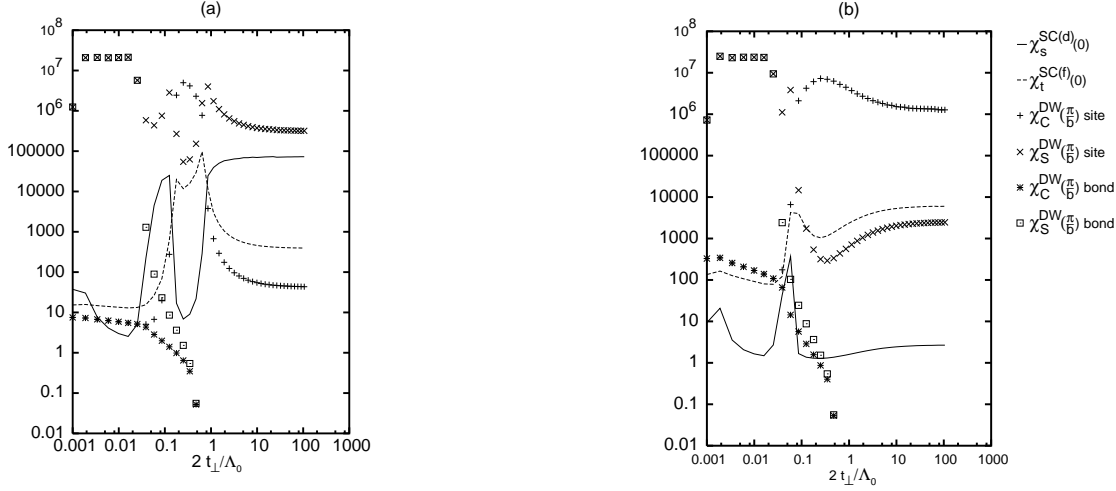


Figure 15: Curves of the susceptibilities (c) versus $2t_2 = 0$, for : a) $C_{back} = 0.4$; b) $C_{back} = 0.6$.

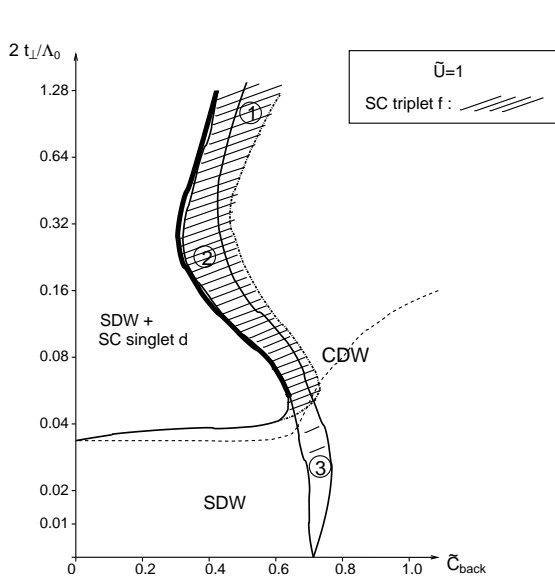


Figure 16: Phase diagram for $U = 1$. The shaded area indicates the divergence of the triplet susceptibility. The dashed line separates site/bond degenerated states (below) and non degenerated ones (above). Other lines and domains are explained in the legend or in the text.

2. Influence of a forward interchain scattering

The phase diagram when C_{for} is included is very rich, and beyond the scope of this article.

We would like to emphasize only the fact that all SC instabilities are suppressed when C_{for} is increased. Fig. 17 gives a typical flow of the susceptibilities, with a large C_{for} .

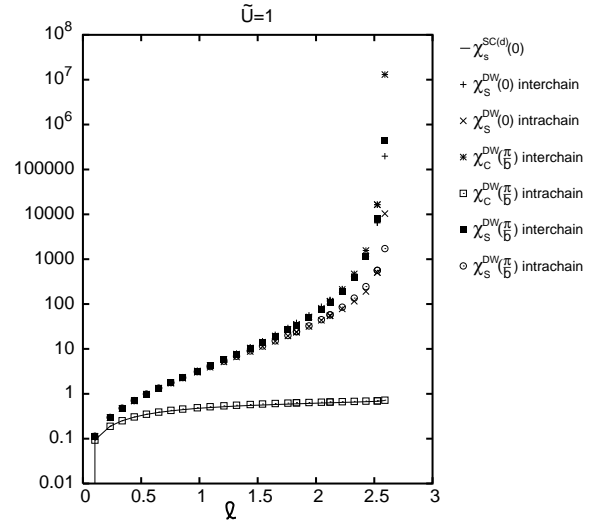


Figure 17: Flow of the susceptibilities, $t_2 = 0.02$ and : $C_{for} = 0.95$.

b. Discussion

Let us analyze these behaviors, which follow simple trends.

The CDW instabilities are enhanced when g_C is increased, whereas SDW ones are enhanced when g_S is increased (this can be verified in the corresponding RG equations of B b). Similarly, singlet SC instabilities are enhanced when g_S is increased, whereas triplet ones are enhanced when g_t is increased.

So, an increase of C_{back} implies an increase of the real space coupling g_1 , and thus, from Eq. (5), it favors CDW instabilities against SDW ones, and from Eq. (4), it favors triplet SC instabilities and depresses singlet SC ones.

Similarly, an increase of C_{for} implies an increase of the

real space coupling g_2 , and thus, from Eq. (5), it favors CDW and SDW instabilities, and from Eq. (4), it depresses SC ones.

Of course, we examine here the influence of parameters C_{back} and C_{back} on the bare couplings. However, we believe that the flow could not just simply reverse this influence, even if the renormalized values of the couplings differ a lot from their bare values. Moreover, one verifies that these conclusions exactly correspond to the observed behaviour.

The density wave interactions are on site, whereas the SC pairing are inter-site (except for singlet s one), so we believe that the DW instabilities appear first, and then enhance the SC ones. This is not true of the DW bond correlations, but we observed no divergences of these ones, and we have not studied any other sophisticated inter-site DW excitation response.

From this point of view, the fact that DW processes are favored, as we already discussed before, implies a dephasing between both chains of the ladder. The dephasing of the SDW thus fits perfectly singlet d condensate (which consists in a pairing of two electrons on a rung, with opposite spins, see Fig. 3 (b)). This accounts nicely for the appearance of singlet SC instability, induced by SDW one.

In the same trend of ideas, the dephasing of the CDW fits triplet f_x condensate (which consists in a pairing of two electrons on each chain, one stepped by unity from the other, see Fig. 4 (a)) and accounts for the appearance of triplet SC instability, induced by CDW one.

On the contrary, the triplet p_x condensate consists in two following electrons on one chain (see Fig. 4 (b)), this pairing is not enhanced by CDW instabilities; in fact, it is the analog of singlet s condensate, which is not either enhanced by SDW instabilities, and is therefore disadvantaged, compared to d pairing.

As can be observed on Fig. 4, triplet f_x condensate are not incompatible with CDW. For instance, one could easily figure out a succession of condensate, with alternate spins, inducing back a global modulation of the chains. A similar scenario is not possible with triplet p condensate.

One should be aware that the symmetry classification we have used is very specific of the ladder system, and could not be extended to an infinite number of chains. The difference between p and f condensate is very subtle and the situation could reveal quite different in the general quasi-one-dimensional systems.

7. CONCLUSION

We have investigated the phase diagram of a ladder system, in the Hubbard model, with an interchain coupling t_\perp , using functional RG method, in the OPI scheme. We have introduced an original parameterization of the k_k dependence, and obtained rather new results, in particular, we have proved the existence of a new phase with only SDW fluctuations, for small enough

values of t_\perp . From the divergences of the scattering couplings, we induce that this phase is different from the one-dimensional solution. However, for very small values of t_\perp ($t_\perp < 0.10^{-4}$), we find the usual one-dimensional behaviour.

Our results altogether prove that the k_k dependence is important and must be taken into account in such a ladder system. The fact that these variables become irrelevant in a ladder does not mean that the corresponding couplings $g(2k_F; 2k_F; 0)$, etc., are relevant. In fact, if the cut-off $\rightarrow 0$, these couplings are left out of the integrated band, so they could only be marginal [28]. However, the divergence takes place at ω_c , which is of the order of k_F , and this explains why these couplings, which are shifted by $2k_F$ from the Fermi points, have a non trivial behaviour and have to be taken into account. Moreover, as already explained in 4b1, during the flow, these couplings influence those, with all momenta at the Fermi points, until $\omega = 2k_F$. This influence is still sensitive, when the divergence takes place. This explains why we could distinguish a new phase, which has not yet been observed by usual methods.

When t_\perp is very large, however (for instance, $t_\perp \rightarrow 0$), the flow continues up to $\omega_c = v_F k_F$ (otherwise, the integrated band would not vary much and the renormalized couplings neither differ much from their bare values), and the above argument applies, proving that couplings $g(2k_F; 2k_F; 0)$, etc., are marginal or irrelevant. In that case, k_k are not irrelevant, and our results coincide indeed with former calculations.

We have also given a detailed classification of the response function, which provides a convenient tool for the determination of order parameters and of related susceptibilities, corresponding to different instability processes.

We are proceeding now to a complete study of the long range correlations, and in particular, of the uniform susceptibility. This task however proves quite difficult, because of the k_k dependence, which has to be carefully taken into account. We expect that the spin-gap will indeed disappear in the SDW phase we have brought to evidence.

We have also investigated the influence of interchain scattering, and showed that a backward interchain scattering can raise triplet superconductivity, a result consistent with the conclusions of a previous work by Bourbonnais et al. [29, 30] on correlated quasi-one-dimensional metals. The appearance of triplet SC in a ladder is a very exciting and promising result, since various authors [40, 41] claim to have found experimental evidence of these instabilities. Even the narrowness of the triplet SC existence region seems to fit the experimental data, which report high sensitivity of these fluctuations to some key parameters. This work gains to be compared with the previous work of Varn et al., who did similar investigations [42].

We would like to thank N. Dupuis, S. Haddad and B. Douçot for fruitful discussions and advices. J. C. N. Ickel

wishes to thank the Gottlieb Daimler- und Karl Benz-Stiftung for partial support.

Appendix

A. Couplings

a. Two-particle couplings

Here are the definitions of the different couplings g , from the two-particle parameter G , and the corresponding diagrams.

$$\begin{aligned}
 g_0(p_1; p_2; p_2^0; p_1^0) &= G(k_{f0} + p_1; k_{f0} + p_2; k_{f0} + p_2^0; k_{f0} + p_1^0) \\
 g(p_1; p_2; p_2^0; p_1^0) &= G(k_f + p_1; k_f + p_2; k_f + p_2^0; k_f + p_1^0) \\
 g_{f0}(p_1; p_2; p_2^0; p_1^0) &= G(k_{f0} + p_1; k_f + p_2; k_f + p_2^0; k_{f0} + p_1^0) \\
 g_f(p_1; p_2; p_2^0; p_1^0) &= G(k_f + p_1; k_{f0} + p_2; k_{f0} + p_2^0; k_f + p_1^0) \\
 g_{t0}(p_1; p_2; p_2^0; p_1^0) &= G(k_{f0} + p_1; k_{f0} + p_2; k_f + p_2^0; k_{f0} + p_1^0) \\
 g_t(p_1; p_2; p_2^0; p_1^0) &= G(k_f + p_1; k_f + p_2; k_{f0} + p_2^0; k_{f0} + p_1^0) \\
 g_{b0}(p_1; p_2; p_2^0; p_1^0) &= G(k_{f0} + p_1; k_f + p_2; k_{f0} + p_2^0; k_f + p_1^0) \\
 g_b(p_1; p_2; p_2^0; p_1^0) &= G(k_f + p_1; k_{f0} + p_2; k_f + p_2^0; k_{f0} + p_1^0)
 \end{aligned}$$

Figure 18: Schematic definitions of the couplings g

The relations between the different representations can be found in Refs. [27] or [43]. Here, they reduce to :

$$\begin{aligned}
 g_s &= g_1 - g_2 & g_c &= g_2 - 2g_1 \\
 g_t &= g_1 - g_2 & g_s &= g_2
 \end{aligned}
 \quad (4) \quad (5)$$

b. Other couplings

Here are the definitions of the different couplings z , from the couplings to external fields Z .

We omit the spin index nor the symmetry index, and use the notation explained further in appendix C a. Mind that $s; d; g$ for s (singlet) and $p; f$ for t (triplet). The symmetry (s, d, g, p, f) applying to each one is detailed in the main text.

$$\begin{aligned}
 z_0^{SC}(p_1; p_2; q) &= Z^{SC}(k_{f0} + p_1; k_{f0} + p_2; (q; 0); 0) \\
 z_+^{SC}(p_1; p_2; q) &= Z^{SC}(k_f + p_1; k_f + p_2; (q; 0);) \\
 z_+^{SC}(p_1; p_2; q) &= Z^{SC}(k_f + p_1; k_{f0} + p_2; (q; \frac{1}{b}); 0) \\
 z_+^{SC}(p_1; p_2; q) &= Z^{SC}(k_{f0} + p_1; k_f + p_2; (q; \frac{1}{b});) \\
 z_0^{DW}(p_1; p_2; q) &= Z^{DW}(k_{f0} + p_1; k_{f0} + p_2; (q - 2k_{f0}; 0); 0) \\
 z_+^{DW}(p_1; p_2; q) &= Z^{DW}(k_f + p_1; k_f + p_2; (q - 2k_f; 0);) \\
 z_+^{DW}(p_1; p_2; q) &= Z^{DW}(k_f + p_1; k_{f0} + p_2; (q - k_{f0} - k_f; \frac{1}{b}); 0) \\
 z_+^{DW}(p_1; p_2; q) &= Z^{DW}(k_{f0} + p_1; k_f + p_2; (q - k_{f0} - k_f; \frac{1}{b});)
 \end{aligned}$$

Figure 19: Schematic definitions of the couplings z

B. RG equations

We give here the detailed RG equations.

a. g couplings

$$P_1 = \begin{pmatrix} 2 & 1 \\ 1 & 0 \end{pmatrix} \quad P_2 = \begin{pmatrix} 0 & 0 \\ 0 & 1 \end{pmatrix};$$

Here are the RG equations for the couplings g , in $(c;l;p)$ representation.

The spin dependence is given, for all terms, by

$$\frac{dg}{d\lambda} = \sum_i g_i C_i + P_i g$$

where C and P correspond, respectively, to the Cooper and Peierls channels, and are given, in the g -ology representation, by

$$C_1 = \begin{pmatrix} 0 & 1 \\ 1 & 0 \end{pmatrix} \quad C_2 = \begin{pmatrix} 1 & 0 \\ 0 & 1 \end{pmatrix}$$

see, for instance, Refs. [27, 43, 44]. In the following equations, all two first terms are Cooper ones, whereas all two last terms are Peierls ones; so, we omit the spin dependence, which is given by the above equations, for each term. One gets

$$\begin{aligned} \frac{dg_0}{d\lambda}(c;l;p) = & \frac{1}{8+4j^2j} \left(\mathcal{G}_0(c; (+\frac{j^2j}{2})+\frac{1+p}{2}; (+\frac{j^2j}{2})+\frac{1+p}{2}) \mathcal{G}_0(c; (+\frac{j^2j}{2})+\frac{1-p}{2}; (+\frac{j^2j}{2})-\frac{1-p}{2}) \right. \\ & + \left. \mathcal{G}_{t0}(c; (+\frac{j^2j}{2})+\frac{1+p}{2}; (+\frac{j^2j}{2})+\frac{1+p}{2}) \mathcal{G}_t(c; (+\frac{j^2j}{2})+\frac{1-p}{2}; (+\frac{j^2j}{2})-\frac{1-p}{2}) \right) \\ & + \frac{1}{8+4jpj} \left(\mathcal{G}_0((+\frac{jpj}{2})+\frac{c+1}{2}; (+\frac{jpj}{2})+\frac{c+1}{2}) \mathcal{G}_0((+\frac{jpj}{2})+\frac{c-1}{2}; (+\frac{jpj}{2})-\frac{c-1}{2}) \right) \\ & + \frac{1}{8+4jp+2k_{\text{eff}}j} \left(\mathcal{G}_{b0}((+\frac{jp+2k_{\text{eff}}j}{2})+\frac{c+1}{2}; k_{\text{eff}}; (+\frac{jp+2k_{\text{eff}}j}{2})+\frac{c-1}{2}; k_{\text{eff}}) \right. \\ & \left. \mathcal{G}_b((+\frac{jp+2k_{\text{eff}}j}{2})+\frac{c-1}{2}; k_{\text{eff}}; (+\frac{jp+2k_{\text{eff}}j}{2})-\frac{c-1}{2}; k_{\text{eff}}) \right) \end{aligned}$$

$$\begin{aligned} \frac{dg_{\text{f}0}}{d\lambda}(c;l;p) = & \frac{1}{8+4j^2j} \left(\mathcal{G}_{\text{f}0}(c; (+\frac{j^2j}{2})+\frac{1+p}{2}; (+\frac{j^2j}{2})+\frac{1+p}{2}) \mathcal{G}_{\text{f}0}(c; (+\frac{j^2j}{2})+\frac{1-p}{2}; (+\frac{j^2j}{2})-\frac{1-p}{2}) \right. \\ & + \left. \mathcal{G}_{b0}(c; (+\frac{jp+2k_{\text{eff}}j}{2})+\frac{1+p}{2}; k_{\text{eff}}; (c+\frac{jp+2k_{\text{eff}}j}{2})+\frac{1-p}{2}; k_{\text{eff}}) \right) \\ & + \frac{1}{8+4jpj} \left(\mathcal{G}_b(c+2k_{\text{eff}}; (+\frac{jp+2k_{\text{eff}}j}{2})+\frac{1-p}{2}; k_{\text{eff}}; (+\frac{jp+2k_{\text{eff}}j}{2})-\frac{1-p}{2}; k_{\text{eff}}) \right. \\ & + \left. \mathcal{G}_{\text{f}0}((+\frac{jpj}{2})+\frac{c+1}{2}; (+\frac{jpj}{2})+\frac{c+1}{2}) \mathcal{G}_{\text{f}0}((+\frac{jpj}{2})+\frac{c-1}{2}; (+\frac{jpj}{2})-\frac{c-1}{2}) \right) \\ & + \mathcal{G}_{t0}((+\frac{jpj}{2})+\frac{c+1}{2}; (+\frac{jpj}{2})+\frac{c+1}{2}) \mathcal{G}_t((+\frac{jpj}{2})+\frac{c-1}{2}; (+\frac{jpj}{2})-\frac{c-1}{2}) \end{aligned}$$

$$\begin{aligned} \frac{dg_{t0}}{d\lambda}(c;l;p) = & \frac{1}{8+4j^2j} \left(\mathcal{G}_0(c; (+\frac{j^2j}{2})+\frac{1+p}{2}; (+\frac{j^2j}{2})+\frac{1+p}{2}) \mathcal{G}_{t0}(c; (+\frac{j^2j}{2})+\frac{1-p}{2}; (+\frac{j^2j}{2})-\frac{1-p}{2}) \right. \\ & + \left. \mathcal{G}_{t0}(c; (+\frac{j^2j}{2})+\frac{1+p}{2}; (+\frac{j^2j}{2})+\frac{1+p}{2}) \mathcal{G}_t(c; (+\frac{j^2j}{2})+\frac{1-p}{2}; (+\frac{j^2j}{2})-\frac{1-p}{2}) \right) \\ & + \frac{1}{8+4jpj} \left(\mathcal{G}_{t0}((+\frac{jpj}{2})+\frac{c+1}{2}; (+\frac{jpj}{2})+\frac{c+1}{2}) \mathcal{G}_{\text{f}0}((+\frac{jpj}{2})+\frac{c-1}{2}; (+\frac{jpj}{2})-\frac{c-1}{2}) \right. \\ & + \left. \mathcal{G}_{\text{f}0}((+\frac{jpj}{2})+\frac{c+1}{2}; (+\frac{jpj}{2})+\frac{c+1}{2}) \mathcal{G}_{t0}((+\frac{jpj}{2})+\frac{c-1}{2}; (+\frac{jpj}{2})-\frac{c-1}{2}) \right) \end{aligned}$$

$$\begin{aligned}
\frac{dg_{b0}}{d\Lambda} (c; l; p) = & \frac{1}{8+4jc_j} \mathcal{G}_{f0} (c; (+\frac{jc_j}{2}) + \frac{1+p}{2} + k_f; (+\frac{jc_j}{2}) + \frac{1+p}{2} + k_f) \mathcal{G}_{b0} (c; (+\frac{jc_j}{2}) + \frac{1-p}{2} - k_f; (+\frac{jc_j}{2}) - \frac{1-p}{2} - k_f) \\
& + \frac{1}{8+4jc_j+2k_{fj}} \mathcal{G}_{b0} (c; (+\frac{jc+2k_{fj}}{2}) + \frac{1+p}{2}; (+\frac{jc+2k_{fj}}{2}) + \frac{1+p}{2}) \mathcal{G}_{f0} (c+2k_f; (+\frac{jc+2k_{fj}}{2}) - \frac{1-p}{2}; (+\frac{jc+2k_{fj}}{2}) - \frac{1-p}{2}) \\
& + \frac{1}{8+4jp_j} \mathcal{G}_{f0} ((+\frac{jp_j}{2}) + \frac{c+1}{2} + k_f; (+\frac{jp_j}{2}) + \frac{c+1}{2} + k_f; p) \mathcal{G}_{b0} ((+\frac{jp_j}{2}) + \frac{c-1}{2} - k_f; (+\frac{jp_j}{2}) - \frac{c-1}{2} - k_f; p) \\
& + \frac{1}{8+4jp+2k_{fj}} \mathcal{G}_{b0} ((+\frac{jp+2k_{fj}}{2}) + \frac{c+1}{2}; (+\frac{jp+2k_{fj}}{2}) + \frac{c+1}{2}; p) \mathcal{G}_{f0} ((+\frac{jp+2k_{fj}}{2}) + \frac{c-1}{2}; (+\frac{jp+2k_{fj}}{2}) - \frac{c-1}{2}; p+2k_f)
\end{aligned}$$

b. z couplings

Charge/Spin representation ($= C; S$). Then, the spin dependence simply writes, for each one

Here are the RG equations for the couplings z , in $(k; c; p)$ representation. The z^{SC} couplings should be written in the singlet/triplet representation ($= s; t$), and the z^{DW} couplings should be written in the

$$\frac{dz}{d\Lambda} = g z$$

and will therefore be again omitted. One gets

$$\begin{aligned}
\frac{dz_0^{SC}}{d\Lambda} (c; k) = & \frac{1}{4+2jc_j} \mathcal{G}_{f0} (c; (+\frac{jc_j}{2}) + \frac{c}{2} - k; (+\frac{jc_j}{2}) + \frac{c}{2} - k) z_0^{SC} (c; (+\frac{jc_j}{2}) + \frac{c}{2}) \\
& + \mathcal{G}_{t0} (c; (+\frac{jc_j}{2}) + \frac{c}{2} - k; (+\frac{jc_j}{2}) + \frac{c}{2} - k) z^{SC} (c; (+\frac{jc_j}{2}) + \frac{c}{2})
\end{aligned}$$

$$\begin{aligned}
\frac{dz_+^{SC}}{d\Lambda} (c; k) = & \frac{1}{4+2jc_j} \mathcal{G}_{f0} (c; (+\frac{jc_j}{2}) + \frac{c}{2} - k; (+\frac{jc_j}{2}) + \frac{c}{2} - k) z_+^{SC} (c; (+\frac{jc_j}{2}) + \frac{c}{2}) \\
& + \frac{1}{4+2jc_j+2k_{fj}} \mathcal{G}_{b0} (c; (+\frac{jc+2k_{fj}}{2}) + \frac{c}{2} - k_f - k; (+\frac{jc+2k_{fj}}{2}) + \frac{c}{2} - k_f - k) z^{SC} (c+2k_f; (+\frac{jc+2k_{fj}}{2}) + \frac{c}{2} - k_f)
\end{aligned}$$

$$\begin{aligned}
\frac{dz_0^{DW}}{d\Lambda} (p; k) = & \frac{1}{4+2jp_j} \mathcal{G}_{f0} ((+\frac{jp_j}{2}) + \frac{p}{2} + k; (+\frac{jp_j}{2}) - \frac{p}{2} - k; p) z_0^{DW} (p; (+\frac{jp_j}{2}) - \frac{p}{2}) \\
& + \frac{1}{4+2jp+2k_{fj}} \mathcal{G}_{b0} ((+\frac{jp+2k_{fj}}{2}) + \frac{p}{2} + k_f + k; (+\frac{jp+2k_{fj}}{2}) - \frac{p}{2} + k_f - k; p+2k_f; (+\frac{jp+2k_{fj}}{2}) - \frac{p}{2} - k_f)
\end{aligned}$$

$$\begin{aligned}
\frac{dz_+^{DW}}{d\Lambda} (p; k) = & \frac{1}{4+2jp_j} \mathcal{G}_{f0} ((+\frac{jp_j}{2}) + \frac{p}{2} + k; (+\frac{jp_j}{2}) - \frac{p}{2} - k; p) z_+^{DW} (p; (+\frac{jp_j}{2}) - \frac{p}{2}) \\
& + \mathcal{G}_{t0} ((+\frac{jp_j}{2}) + \frac{p}{2} + k; (+\frac{jp_j}{2}) - \frac{p}{2} - k; p) z^{DW} (p; (+\frac{jp_j}{2}) - \frac{p}{2})
\end{aligned}$$

c. couplings

Here are the RG equations for the susceptibilities, with the same spin dependence as the corresponding z couplings, which is again omitted,

$$\frac{d\chi_0^{SC}}{d\Lambda} (q) = \frac{1}{4+2jc_j} z_0^{SC} (q; (+\frac{jc_j}{2}) + \frac{q}{2})^2 + z^{SC} (q; (+\frac{jc_j}{2}) + \frac{q}{2})^2$$

$$\frac{d_+^{SC}}{d_+} (q) = \frac{P}{4+2j_1j_2} Z_+^{SC} (q; (+\frac{j_1j_2}{2})+\frac{q}{2})^2 \frac{P}{4+2j_1+2k_{fj}} Z_+^{SC} (q+2k_{fj}; (+\frac{j_1+2k_{fj}}{2})+\frac{q}{2}+k_{fj})^2$$

$$\frac{d_0^{DW}}{d_+} (q) = \frac{P}{4+2j_1j_2} Z_0^{DW} (q; (+\frac{j_1j_2}{2})+\frac{q}{2})^2 \frac{P}{4+2j_1-2k_{fj}} Z_0^{DW} (q+2k_{fj}; (+\frac{j_1-2k_{fj}}{2})+\frac{q}{2}-k_{fj})^2$$

$$\frac{d_-^{DW}}{d_+} (q) = \frac{P}{4+2j_1j_2} Z_+^{DW} (q; (+\frac{j_1j_2}{2})+\frac{q}{2})^2 + \frac{P}{4+2j_1j_2} Z_-^{DW} (q; (+\frac{j_1j_2}{2})+\frac{q}{2})^2$$

C. Symmetries

a. Ordinary symmetries

If we apply the conjugation symmetry C to the two-particle coupling G , we get :

$$G(P_1^0; P_2^0; P_2; P_1) = G(P_1; P_2; P_2^0; P_1^0);$$

if we apply A , we get :

$$\begin{aligned} G_C(P_2; P_1; P_2^0; P_1^0) &= \\ 2G_C(P_1; P_2; P_2^0; P_1^0) - 3G_S(P_1; P_2; P_2^0; P_1^0) &= \\ G_S(P_2; P_1; P_2^0; P_1^0) &= \\ G_C(P_1; P_2; P_2^0; P_1^0) + 2G_S(P_1; P_2; P_2^0; P_1^0); & \end{aligned}$$

if we apply A^0 , we get :

$$\begin{aligned} G_C(P_1; P_2; P_1^0; P_2^0) &= \\ 2G_C(P_1; P_2; P_2^0; P_1^0) - 3G_S(P_1; P_2; P_2^0; P_1^0) &= \\ G_S(P_1; P_2; P_1^0; P_2^0) &= \\ G_C(P_1; P_2; P_2^0; P_1^0) + 2G_S(P_1; P_2; P_2^0; P_1^0); & \end{aligned}$$

and, nally, from parity P conservation, we get

$$G(P_1; P_2; P_2^0; P_1^0) = G(P_1; P_2; P_2^0; P_1^0);$$

Note that AA^0 simply gives $G(P_2; P_1; P_1^0; P_2^0) = G(P_1; P_2; P_2^0; P_1^0)$.

For the SC instability coupling, we will write the two-dimensional interaction vector $Q = (Q_k; Q_?)$, and add a discrete variable $\sigma = 0; \pm$, which indicates whether the R particle is on the 0-band ($\sigma = 0$) or the \pm -band ($\sigma = \pm$); this way, one can distinguish 0-0, 0- \pm , \pm -0 or \pm - \pm processes (use Fig. 2 for help).

If we apply P , we get

$$Z^{SC}(P_1; P_2; (Q_k; Q_?); \sigma) = Z^{SC}(P_1; P_2; (Q_k; Q_?); -\sigma);$$

if we apply A or A^0 (note that in H_{SC} , the term with incoming momenta P_1 and P_2 is conjugate to that with outgoing momenta P_1 and P_2), we get

$$\begin{aligned} Z^{SC}(P_2; P_1; (Q_k; 0); \sigma) &= Z^{SC}(P_1; P_2; (Q_k; 0); \sigma) = s; t \\ Z_s^{SC(s)}(P_2; P_1; (Q_k; \frac{Q_?}{b}; Q_?); \sigma) &= Z_s^{SC(s)}(P_1; P_2; (Q_k; Q_?); \sigma) \\ Z_s^{SC(g)}(P_2; P_1; (Q_k; \frac{Q_?}{b}; Q_?); \sigma) &= Z_s^{SC(g)}(P_1; P_2; (Q_k; Q_?); \sigma) \\ Z_t^{SC(p_x)}(P_2; P_1; (Q_k; \frac{Q_?}{b}; Q_?); \sigma) &= Z_t^{SC(p_x)}(P_1; P_2; (Q_k; Q_?); \sigma) \\ Z_t^{SC(f_y)}(P_2; P_1; (Q_k; \frac{Q_?}{b}; Q_?); \sigma) &= Z_t^{SC(f_y)}(P_1; P_2; (Q_k; Q_?); \sigma); \end{aligned}$$

Finally, it is interesting to note that Z_s^{SC} (singlet) and $Z_{t_x}^{SC}$ (triplet) change sign under S and are invariant under C , while $Z_{t_y}^{SC}$ and $Z_{t_z}^{SC}$ (both triplet) do the opposite.

For the DW instability coupling, we use the same notation. Note that Q_k writes

$(q - p + 2k_f)$ for intraband processes, and $(q - p + k_{f0} + k_f)$ for interband ones. If we apply CS , we get :

$$\begin{aligned} Z^{DW}(P_1; P_2; (2k_f - Q_k; Q_?); \sigma) &= \\ Z^{DW}(P_1; P_2; (2k_f + Q_k; Q_?); -\sigma); & \end{aligned}$$

and if we apply AS , we get

$$\begin{aligned} Z^{DW}(P_2; P_1; (2k_f - Q_k; Q_?); \sigma) &= \\ Z^{DW}(P_1; P_2; (2k_f + Q_k; Q_?); -\sigma); & \end{aligned}$$

$$\begin{aligned} Z^{DW}(P_2; P_1; (k_{f0} + k_f - Q_k; \frac{Q_?}{b}; Q_?); \sigma) &= \\ Z^{DW}(P_1; P_2; (k_{f0} - k_f + Q_k; Q_?); -\sigma); & \end{aligned}$$

where σ reads $+$ for site ordering, and $-$ for bond ordering.

b. Supplementary symmetry

When we apply the special symmetry \tilde{C} to two-particle couplings G , we get :

$$G(k_{f0} + k_f, P_1; k_{f0} + k_f, P_2; k_{f0} + k_f, P_2^0; k_{f0} + k_f, P_1^0) = G(P_1; P_2; P_2^0; P_1^0)$$

When we apply the special symmetry \tilde{C} to SC instabilities Z_{SC} , we get :

$$\begin{aligned} Z^{SC(\cdot)}(k_{f0}, k_f, P_1; k_{f0} + k_f, P_2; (Q_k; 0);) &= \tilde{Z}^{SC(\cdot)}(P_1; P_2; (Q_k; 0);) \\ Z^{SC(\cdot)}(k_{f0}, k_f, P_1; k_{f0} + k_f, P_2; (Q_k; \frac{1}{b}, Q_?);) &= \tilde{Z}^{SC(\cdot)}(P_1; P_2; (Q_k; Q_?);) \end{aligned}$$

where reads + for = s, = s or for = t, = p_x, and for = s, = d; g or for = t, = f_x; f_y.

When we apply the special symmetry \tilde{C} to DW instabilities Z_{DW} , we get :

$$Z^{DW}(k_{f0}, k_f, P_1; k_{f0} + k_f, P_2; (2k_f, Q_k; 0);) = \tilde{Z}^{DW}(P_1; P_2; (2k_f, Q_k; 0);)$$

$$Z^{DW}(k_{f0}, k_f, P_1; k_{f0} + k_f, P_2; (k_{f0}, k_f, Q_k; \frac{1}{b}, Q_?);) = \tilde{Z}^{DW}(P_1; P_2; (k_{f0}, k_f + Q_k; Q_?);)$$

where reads + for site ordering, and for bond ordering.

c. g_{b0} orbits

Here are the 8 first orbits of the g_{b0} coefficient, in (c;l;p) representation :

$$\begin{aligned} f(0; 0; 2k_f; 0); (0; 2k_f; 0); (2k_f; 0; 0); (2k_f; 2k_f; 2k_f) &\text{g are sym. equiv.} \\ f(4k_f; 4k_f; 2k_f); (4k_f; 2k_f; 0); (2k_f; 4k_f; 0); (2k_f; 2k_f; 2k_f) &\text{g id.} \\ f(0; 4k_f; 2k_f); (0; 2k_f; 4k_f); (2k_f; 4k_f; 4k_f); (2k_f; 2k_f; 2k_f) &\text{g id.} \\ f(4k_f; 0; 2k_f); (4k_f; 2k_f; 4k_f); (2k_f; 0; 4k_f); (2k_f; 2k_f; 2k_f) &\text{g id.} \\ f(0; 4k_f; 2k_f); (0; 2k_f; 0); (2k_f; 4k_f; 0); (2k_f; 2k_f; 2k_f) &\text{g id.} \\ f(4k_f; 0; 2k_f); (4k_f; 2k_f; 0); (2k_f; 0; 0); (2k_f; 2k_f; 2k_f) &\text{g id.} \\ f(0; 0; 2k_f); (0; 2k_f; 4k_f); (2k_f; 0; 4k_f); (2k_f; 2k_f; 2k_f) &\text{g id.} \\ f(4k_f; 4k_f; 2k_f); (4k_f; 2k_f; 4k_f); (2k_f; 4k_f; 4k_f); (2k_f; 2k_f; 2k_f) &\text{g id.} \end{aligned}$$

D. Fourier Transform

Creation and annihilation operators If one writes \hat{c}_{ij}^y the creator of a particle of spin y , located in real space at position i ($i \in \mathbb{Z}$); N g), on chain j ($j = 1$), the representation in the momentum space writes

$$\begin{aligned} L_{p;0} &= (k_{f0} + p; 0) = \sum_{ij} c_{ij} e^{-(p + k_{f0})ia} \\ L_{p; \frac{1}{b}} &= (k_f + p; \frac{1}{b}) = \sum_{ij} c_{ij} e^{-(p + k_f)ia} \end{aligned}$$

$$\begin{aligned} R_{p;0} &= (k_{f0} + p; 0) = \sum_{ij} c_{ij}^{\dagger} e^{-(p + k_{f0})ia} \\ R_{p; \frac{1}{b}} &= (k_f + p; \frac{1}{b}) = \sum_{ij} c_{ij}^{\dagger} e^{-(p + k_f)ia} \end{aligned}$$

with the notations of the text. k stands for the absolute momentum representation, while L and R stand for the relative momentum representation. These relations are given for annihilation operators, one must take the complex conjugation to obtain those for the creation operators.

The reverse relations simply write, in terms of the

operators,

$$ij = \sum_a \frac{adP}{4} e^{aip} ((P;0)_i + j (P;\bar{a})_i);$$

but one can also express them in terms of the L and R operators. Then, one can check that this transformation is the inverse of the first one.

Electron-electron pair operator In real space, the SC order parameters are the mean value of the electron-electron pair operator, which writes

$$O(X) = \sum_{x=0}^X X_{x=0} (X;X^0)_{x=0} :$$

To each $Q = (Q_k; Q_?)$ corresponds a Fourier component

$$O(Q) = \sum_X e^{Q \cdot X} O(X) = \sum_{ij} e^{-(aQ_k i + bQ_? j=2)} O(X) :$$

We only keep the components Q which lead to singularities; as explained in the main text, they are $(0;0)$ and $(k_f; \frac{a}{b})$. So, using the short notation O for the first and \bar{O} for the second, one gets

$$O(0) = \sum_i O(ai;1) + O(ai; \bar{1})$$

and

$$O(k_f) = \sum_i e^{-k_f a} O(ai;1) - O(ai; \bar{1})$$

where the main factor $O(ai;1) - O(ai; \bar{1}) = \sum_{jj^0} (1)^j_{ij} i^0 j^0_{i^0} (a(i i^0); b(j j^0)=2)_{i^0}$ is the mixed representation of the pair operator[45].

Eventually, the ij can be expressed in terms of the P , so that the components write

$$O(Q) = \sum_a \frac{adP}{4} \sum_X Z_Q(P) \sum_{p; Q-P; 0} X_{p; Q-P; 0} = 0;$$

where $p = (P; \frac{a}{b})$ and we will also use $Q = (Q_k; Q_?)$. Be careful that, for instance, with $Q = (k_f; \frac{a}{b})$ and $p = (p_{k_f 0}; 0)$, and thus $p; = L_{p;0}$, the calculation of $Q_{p; 0}$ is not immediate; one gets $Q_{p; 0} = (k_f + p_{k_f 0}; \frac{a}{b})_{i^0} = R_{2k_f p; i^0}$.

With $(X; X^0) = i i^0 j j^0$, one finds $z_0(p) = 1$ (singlet 0-condensate of s symmetry), and $z(p) = -$ (singlet -condensate of s symmetry). With $(X; X^0) = i i^0 j; j^0$, one finds $z_0(p) = \cos(\)$ (singlet 0-condensate of d symmetry) and $z(p) = -\cos(\)$ (triplet -condensate of f_y symmetry). With $(X; X^0) = i i^0 1 j; j^0$, one finds $z_0(p) = \cos(aP) \cos(\)$ (singlet 0-condensate of extended d symmetry), as well as $z_0(p) = -\sin(aP) \cos(\)$ (triplet 0-condensate of f_x symmetry), and $z(p) = \sin(a(P - \frac{k_f a}{2})) \cos(\)$ (singlet -condensate of g symmetry) or $z(p) = -e^{-\frac{k_f a}{2}} \cos(a(P - \frac{k_f a}{2})) \cos(\)$ (triplet -condensate of extended f_y symmetry). With

$(X; X^0) = i i^0 1 j j^0$, one finds $z_0(p) = \cos(aP)$ (singlet 0-condensate of extended s symmetry) or $z_0(p) = -\sin(aP)$ (triplet 0-condensate of p symmetry), and $z(p) = -e^{-\frac{k_f a}{2}} \cos(a(P - \frac{k_f a}{2}))$ (singlet -condensate of extended s symmetry) or $z(p) = e^{-\frac{k_f a}{2}} \sin(a(P - \frac{k_f a}{2}))$ (triplet -condensate of p_x symmetry).

Electron-hole pair operator It is almost the same, with the product of a creation and an annihilation operators, be careful, however, that, in reciprocal space, one gets :

$$X \sum_a \frac{adP}{4} \sum_{p; Q+p; 0} Y_{p; Q+p; 0} Z(P)_{i^0} :$$

- [1] M. A. zum a, Z. Hiroi, M. Takano, K. Ishida & Y. Kitaoka, Phys. Rev. Lett. 73, 3463 (1994).
- [2] Le Carron, Mater. Res. Bull. 23, 1355 (1988); Sigrist, ibidem, 1429.
- [3] Z. Hiroi & M. Takano, Nature 377, 41 (1995).
- [4] For a review of experimental results, see E. Dagotto, Rep. Prog. Phys. 62, 1525 (1999).
- [5] K. Penc & J. Solym, Phys. Rev. B 41, 704 (1990).
- [6] T. Giamarchi & H. J. Schulz, J. Phys. (France) 49, 819 (1988).
- [7] M. Tsuchiizu, P. Donohue, Y. Suzumura & T. Giamarchi, Eur. Phys. J. B 19, 185 (2001).
- [8] J. I. Kishine & K. Yonemitsu, J. Phys. Soc. Jpn. 67, 1714 (1998).
- [9] K. Le Hur, Phys. Rev. B 63, 165110 (2001).

- [10] S. Haddad, S. Char-Kaddour, M. Heritier & R. Ben-naceur, J. de Phys. IV (France) 10, 3 (2000).
- [11] E. Dagotto, J. Riera & D. Scalapino, Phys. Rev. B 45, R5744 (1992).
- [12] M. Fabrizio, Phys. Rev. B 48, 15838 (1993).
- [13] D. V. Khvashchenko & T. M. Rice, Phys. Rev. B 50, 252 (1993).
- [14] T. Barnes, E. Dagotto, J. Riera & E. S. Swanson, Phys. Rev. B 47, 3196 (1993).
- [15] H. Lin, L. Balents & M. P. A. Fisher, Phys. Rev. B 56, 6569 (1997).
- [16] A. M. Finkelstein & A. I. Larkin, Phys. Rev. B 47, 10461 (1993).
- [17] H. J. Schulz, Phys. Rev. B 53, R2959 (1996).
- [18] E. Ognac & T. Giamarchi, Phys. Rev. B 56, 7167

- (1997).
- [19] K. Kuroki & H. Aoki, *Phys. Rev. Lett.* 72, 2947 (1994).
 - [20] D. V. Khveshchenko, *Phys. Rev. B* 50, 380 (1993).
 - [21] D. J. Scalapino, *J. Low Temp. Phys.* 117, 179 (1999).
 - [22] R. M. Noack, S. R. White & D. J. Scalapino, *Phys. Rev. Lett.* 73, 882 (1994).
 - [23] J. I. Kishine & K. Yonemitsu, *J. Phys. Soc. Jpn.* 67, 2590 (1998).
 - [24] Y. Park, S. Liang & T. K. Lee, *Phys. Rev. B* 59, 2587 (1999).
 - [25] W. Metzner, C. Castellani & C. Di Castro, *Adv. Phys.* 47, 317 (1998).
 - [26] C. Honerkamp, *Ph.D. Thesis, Naturwissenschaften ETH Zurich*, Nr. 13868 (2000).
 - [27] C. Halboth, *PhD Thesis, RWTH Aachen* (1999).
 - [28] R. Shankar, *Rev. Mod. Phys.* 66, 129 (1994).
 - [29] C. Bourbonnais and R. Duprat, *Bulletin of the American Physical Society*, 49 No. 1, 179 (2004).
 - [30] J. C. Nickel, R. Duprat, C. Bourbonnais & N. Dupuis, *cond-mat/0502614*.
 - [31] S. Dusuel, F. V. de Abreu & B. Doucot, *Phys. Rev. B* 65, 94505 (2002).
 - [32] J. Solym, *Adv. Phys.* 28, 201 (1979).
 - [33] C. Honerkamp, M. Salmhofer, N. Furukawa & T. M. Rice, *Phys. Rev. B* 63, 35109 (2001).
 - [34] B. Binz, D. Baeriswyl & B. Doucot, *Ann. Phys.* 12, 704 (2003).
 - [35] C. Bourbonnais, A renormalization group approach to electronic and lattice correlations in organic conductors, in *Strongly interacting fermions and high- T_c superconductivity* ed. B. Doucot & J. Zinn-Justin, Les Houches LVI (1991), Elsevier Science 1995.
 - [36] V. N. Prigodin & Y. A. Firsov, *Sov. Phys. JETP* 49, 813 (1979).
 - [37] P. A. Lee, T. M. Rice & R. A. Klemm, *Phys. Rev. B* 15, 2984 (1977).
 - [38] V. J. Emery, *Synthetic Metals*, 13 (1986).
 - [39] N. Furukawa, T. M. Rice & M. Salmhofer, *Phys. Rev. Lett.* 81, 3195 (1998).
 - [40] I. J. Lee, P. M. Chaikin & M. J. Naughton, *Phys. Rev. B* 62, R14669 (2000); I. J. Lee, S. E. Brown, W. G. Clark, M. J. Strouse, M. J. Naughton, W. Kang & P. M. Chaikin, *Phys. Rev. Lett.* 88, 17004 (2002); I. J. Lee, D. S. Chow, W. G. Clark, M. J. Strouse, M. J. Naughton, P. M. Chaikin & S. E. Brown, *Phys. Rev. B* 68, 92510 (2003).
 - [41] R. W. Chemg, C. A. R. Sa de Melo, *Phys. Rev. B* 67, 212505 (2002).
 - [42] C. M. Vamra & A. Zawadowski, *Phys. Rev. B* 32, 7399 (1985).
 - [43] J. C. Nickel, *These de troisieme cycle, de l'Universite Paris 11* (2004).
 - [44] D. Zanchi, *Europhys. Lett.* 55, 376 (2001).
 - [45] see, for instance, D. Poilblanc, M. Heritier, G. Montambaux & P. Lederer, *J. Phys. C: Solid State Phys.* 19, L321 (1986).